University of Padova

Department of Physics and Astronomy "Galileo Galilei"

Master Thesis in Astrophysics and Cosmology

Estimating Source of Galactic Neutrinos

Supervisor
Prof. Elisa Bernardini
University of Padova

Co-supervisor
Dr. Kathrin Egberts
University of Potsdam

Master Candidate
Mohadeseh Ozlati Moghadam

Student ID
2009431

Academic Year
2022-2023

"I suppose therefore that all things I see are illusions; I believe that nothing has ever existed of everything my lying memory tells me. I think I have no senses. I believe that body, shape, extension, motion, location are functions. What is there then that can be taken as true? Perhaps only this one thing, that nothing at all is certain."
— Rene Descartes

Abstract

This master's thesis focuses on predicting Galactic neutrino flux which provides valuable insights into the origin of cosmic rays. Neutrinos and gamma rays are expected to be produced simultaneously in proton-proton (pp) interactions. By establishing a correlation between their spectra, we aim to predict potential galactic neutrino emission. We have developed a model that quantifies the relationship between the predicted neutrino fluxes and gamma-ray fluxes with the assumption of a purely hadronic gamma-ray emission. We utilized a synthetic dataset of 3000 very high-energy (VHE) gamma-ray populations to predict neutrino sources in the Milky Way. The populations were a combination of observed and simulated gamma ray sources. Applying our developed model to these sources, we predicted the corresponding Galactic neutrino emissions.

To assess the accuracy of our predictions, we compared the calculated total expected neutrino flux with the diffuse flux observed by IceCube and the upper limit established by ANTARES. Our results indicate that our total predicted neutrino flux from galactic sources is lower than the overall neutrino flux observed by neutirno detectors, as our model specifically focuses on neutrinos originating within our galaxy which is a subset of all the possible sources of neutrinos. Furthermore, we generated sky maps using the Gammapy package in Python to visualize the flux of the predicted sources and their spatial distribution across the galactic plane. Additionally, a comparison with observed neutrino events from the ANTARES neutrino detector was conducted to investigate the correspondence between the predicted sources and observed events. In average, our model predicted 54 counts for ANTARES and 222 counts for KM3NeT which are lower than the 747 actual event counts recorded by ANTARES. This was consistent with our expectations since neutrino detectors, such as ANTARES, detect both astrophysical and atmospheric neutrinos. Moreover, spatial positions of ANTARES events in the galactic plane do not conclusively prove that these events originate from galactic sources.

In conclusion, this thesis centers on predicting Galactic neutrino flux, comparing it with data (e.g., spectrum and Galactic Plane counts), and making projections for future experiments like KM3NeT. Further investigations, including multi-wavelength correlations and advancements in neutrino telescopes, hold great potential for improving our understanding of these sources and unraveling the mysteries of the universe.

Acknowledgments

I would like to express my heartfelt gratitude to the following individuals who played pivotal roles in the completion of this research and the writing of this thesis. Firstly, I extend my deepest appreciation to my supervisors, Dr. Kathrin Egberts and Prof. Elisa Bernardini, whose guidance, expertise, and unwavering support have been invaluable throughout this journey. They have been like role models and a constant source of inspiration to me. I am also grateful to the Experimental Astroparticle Group at the University of Potsdam, particularly Dr. Constantin Steppa, Rowan Batzofin, and Karol Peters, for their collaboration, insightful discussions, and assistance in various aspects of my research.

I would also like to acknowledge Rowan Batzofin and Nukri Komin, the authors of the paper "Predicting Neutrino Emission for the Sources in the H.E.S.S. Galactic Plane Survey,"[1] which served as a foundation for this research. I am particularly grateful to Rowan Batzofin for his invaluable assistance. His extensive knowledge and generosity in sharing his expertise have been instrumental in the success of this research. Furthermore, I am deeply grateful to the University of Padova for their support and funding through my master's study. They also provided me with the opportunity to pursue studies outside of Italy, which has helped me to broaden my horizons and enrich my research experience.

I would like to extend my heartfelt thanks to my family, who have been my pillars of strength, offering unconditional support and encouragement from afar. Their belief in me has been a driving force throughout this journey. I am also thankful to my dear friend, Dr. Victor Mauricio Gomez Gonzalez, for his companionship working alongside me whenever I worked late into the night. I am also indebted to Florian Ruenger, Moritz Itzerott and Sabela Reyero Serantes, for their kindness and emotional support.

To all the individuals mentioned above, as well as those whose names may not be listed here but have contributed to my journey in any way, I extend my deepest appreciation. Your support, encouragement, and guidance have been instrumental in the successful completion of this thesis.

Contents

Listing of figures

1 Introduction

In this thesis, our primary objective is to forecast Galactic neutrino flux, which holds the key to better understanding the origins of cosmic rays. The origin of cosmic rays has yet remains a longstanding challenge, although they have been a subject of scientific inquiry for over a century. This is due to the fact that their trajectory is influenced by magnetic fields, making it more difficult to identify their sources. However, as they propagate through the universe, they produce neutrinos as well as gamma rays. By investigating the sources of neutrinos, we gain valuable insights into potential cosmic ray accelerators and deepen our understanding of particle acceleration mechanisms.

Of particular interest is the phenomenon known as hadronic interaction wherein charged and neutral pions are generated in proton-proton collisions. Charged pions subsequently decay into muons and neutrinos, while neutral pions decay into gamma rays. This simultaneous production of gamma rays and neutrinos presents a unique opportunity for us to probe the origins of cosmic rays. It is important to note that while gamma rays can have both leptonic and hadronic origins, in the case of hadronic processes, they are invariably accompanied by neutrinos. In cases where we can assume a purely hadronic origins for gamma rays, we can thereby study the connections they have with neutrinos.

Building upon the groundbreaking work of Batzofin and Komin in their study titled "Predicting Neutrino Emission for the Sources in the H.E.S.S. Galactic Plane Survey," [1] we have developed a model that predicts neutrino fluxes in the galactic plane. Utilizing their neutrino flux predictions for the H.E.S.S. sources, we determined the fraction of neutrino fluxes relative to gamma-ray fluxes. Through this, we have derived a novel parameterization that establishes a relationship between gamma ray flux and neutrino flux.

To validate the accuracy of our predictions, we have compared our model results with observational data obtained from the ANTARES and made prediction for KM3NeT neutrino telescopes. These telescopes, situated in the Northern hemisphere, provide excellent visibility of the Galactic Plane, making them powerful tools for

studying astrophysical point sources, particularly of Galactic origin. We compared eleven years of ANTARES data (recorded between 2007 and 2017) to compare with our predicted results. By employing the effective area of the telescopes and integrating over the observation time, we have calculated the expected number of neutrino counts for each source in the simulated very high energy (VHE) gamma ray populations.

In summary, this thesis endeavors to identify the sources of galactic neutrinos, a step towards unraveling the origins of cosmic rays. Through the development of a new parameterization linking gamma ray flux to neutrino flux, we predicted potential neutrino sources within our galaxy. By comparing these predictions with data obtained from ANTARES and those predicted for the KM3NeT telescope, we have successfully evaluated the spatial agreement between our model and the observed neutrino events. These findings contribute to our understanding of the astrophysical processes underlying cosmic ray acceleration and shed light on the elusive sources of galactic neutrinos.

The complex nature of cosmic rays and neutrinos calls for continued exploration and investigation. Further analyses and cross-disciplinary collaborations, including multi-wavelength observations, will be instrumental in unraveling the full extent of the cosmic puzzle.

2

Cosmic Rays, Gamma Rays, and Neutrinos

Cosmic rays, which consist mainly of protons and atomic nuclei, have puzzled scientists for decades due to their mysterious origins. As these energetic particles propagate through the universe and interact with interstellar gas and ambient radiation, they give rise to the production of gamma rays and neutrinos. By exploring the connection between these three cosmic messengers, we can unravel the mysteries of the universe and gain deeper insights into the underlying astrophysical mechanisms that drive their production.

In this chapter, I will provide a concise overview of the relevant concepts related to cosmic rays, neutrinos, and gamma rays. I will begin by explaining what cosmic rays are and their significance in astrophysics. Next, I will discuss the unique characteristics of neutrinos and their detection through neutrino telescopes. Following that, I will shift the focus to gamma rays, which are another essential component in this research. I will introduce gamma-ray telescopes and their capabilities in detecting, followed by gamma-ray emissions in leptonic and hadronic scenarios. Building upon this foundation, I will explain how proton-proton ("pp") interactions can give rise to the production of both neutrinos and gamma rays, which form the cornerstone of this research.

2.1 Cosmic rays

Cosmic rays are high-energy radiation comprising charged particles originating in outer space. They continually bombard the Earth from all directions at speeds nearing the speed of light. The majority of cosmic rays are atomic nuclei, ranging from the lightest to the heaviest elements in the periodic table. Less common are high-energy electrons and positrons, among other subatomic particles, and photons. One of the pioneering discoveries in this field can be attributed to Victor Hess, an Austrian physicist, who in 1912 conducted a landmark experiment that changed our understanding of the nature of cosmic rays.

Hess's experiment involved ascending in a balloon equipped with an electroscope, a device used to detect the presence of charged particles. As he climbed higher into the atmosphere, Hess observed that the electroscope discharged more rapidly, indicating the presence of a source of radiation from above. This led him to conclude that the radiation originated from outside the Earth's atmosphere, thus opening up a new frontier of research into the nature and origins of cosmic rays.

Figure 2.1: Historical photograph of Hess preparing for a balloon flight (American Physical Society)

The results by Hess were later confirmed by Kolhörster in a number of flights up to 9200 m. An increase in ionization of up to ten times that at sea level was found (See Figure 2.2). This was a historic discovery in astrophysics which was foundational also for many results in particle physics, such as the discovery of the positron. [7]

2.1.1 Cosmic ray properties

Initially, cosmic rays were believed to be a part of the electromagnetic spectrum; hence "rays". However, it was discovered in the 1930s that cosmic rays must be electrically charged because of their interaction with the Earth's magnetic field. The study of cosmic rays has since been a field of active research, providing valuable insights into the structure and behavior of the universe, and serving as an important tool for the exploration of astrophysics and cosmology.

The detection of cosmic rays across their wide energy spectrum requires the utilization of various types of instruments, balloon-borne experiments like BESS [8], ATIC-2 [9], and CREAM [10], as well as space-based instruments such as PAMELA [11] and AMS [12], all employing direct measurement techniques to allow for highly sensitive measurements of their energies and composition.

In contrast, ground-based experiments like KASCADE [13], the Telescope Array [14], and the Pierre Auger Observatory [15] take advantage of indirect detection methods. They detect cosmic rays by studying the extensive

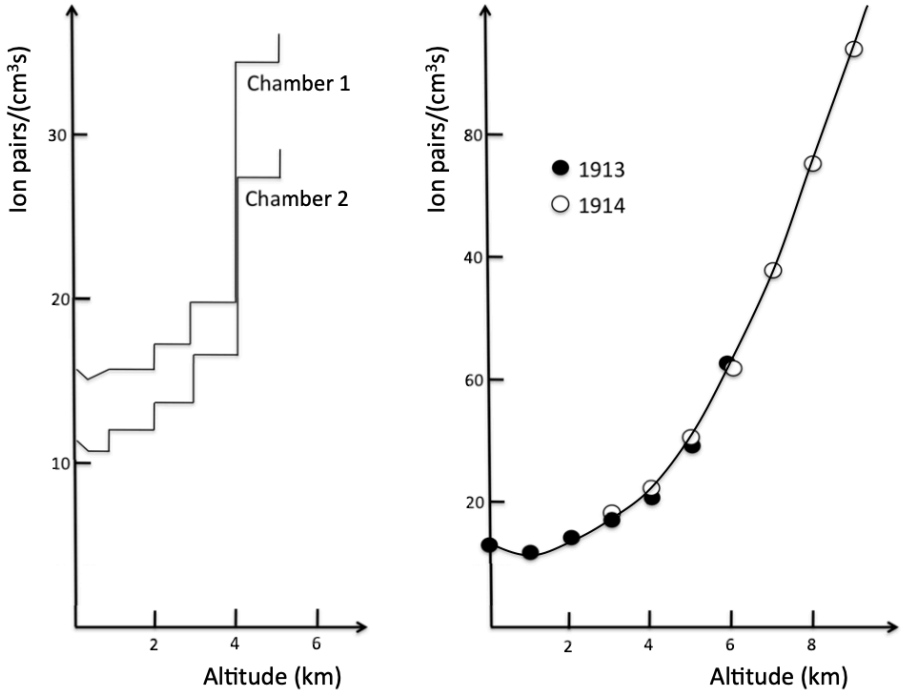

Figure 2.2: Variation of ionization with altitude. Left panel: Final ascent by Hess (1912), carrying two ion chambers. Right panel: Ascents by Kolhörster (1913, 1914). Original drawing by A. De Angelis.

air showers generated when primary cosmic rays interact with the Earth's atmosphere. By observing the secondary particles produced in these air showers, these experiments are able to infer the properties of the primary cosmic rays.

The study of cosmic rays usually involves a detailed analysis of their energy spectrum. The flux of cosmic rays ($d\varphi$) is often expressed as the number of particles (dN) per area (dA), per second (dt), per solid angle ($d\Omega$), and per energy interval (dE).

$$d\varphi = \frac{dN}{dA \cdot dt \cdot d\Omega \cdot dE} \tag{2.1}$$

Cosmic rays are typically observed to exhibit a power law energy spectrum. Figure 2.3 shows the all-particle energy spectrum of cosmic rays obtained by different experiments.

The cosmic ray spectrum exhibits different features at distinct energy ranges (see Figure 2.4). The spectrum can be approximated by a power law of approximately $E^{-2.7}$ up to the so-called "knee", which occurs at an energy of approximately 3 PeV. Beyond this energy, the spectrum changes to a steeper power law of approximately $E^{-3.1}$ before reaching the "ankle" at approximately 5 EeV. Thereafter, the cosmic ray spectrum becomes progressively more difficult to quantify, roughly approximated by the law $E^{-2.7}$.

There is a mixed consensus as to whether it is the knee that marks the transition to where cosmic rays produced

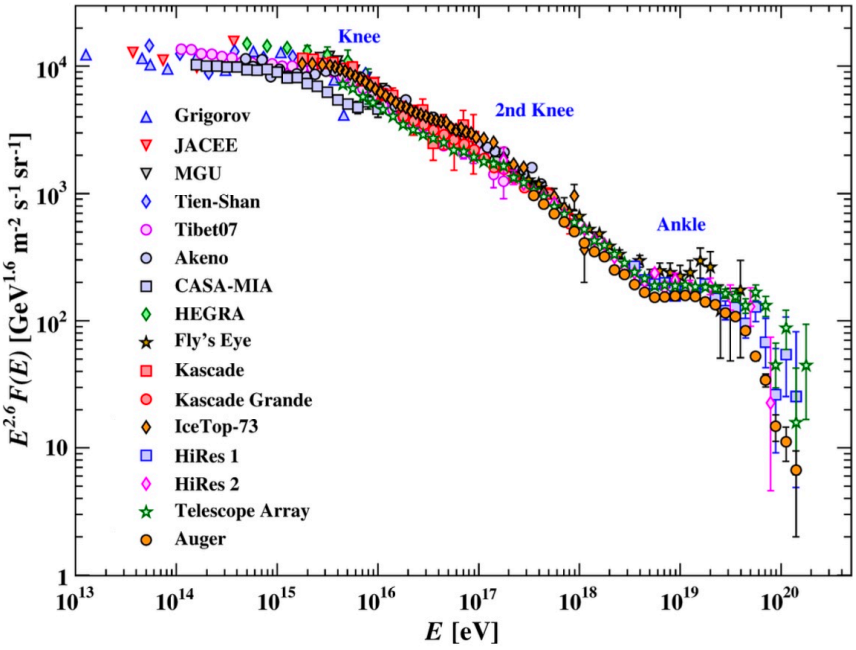

Figure 2.3: All-particle energy spectrum obtained from different experiments. Figure extracted from [2]

by extra-galactic sources dominate over those of galactic and solar origin, or if it is the ankle. Either way, towards the end of the cosmic ray spectrum, there is a significant suppression in the particle flux observed above an energy of 4×10^{19} eV. This observation aligns with the predictions made by Greisen [16] and Zatsepin & Kuz'min [17], known as the GZK effect. According to these predictions, interactions between cosmic rays and photons from the cosmic microwave background (CMB) result in a spectral cut-off at around 6×10^{19} eV due to pion production. However, recent measurements indicate a heavier composition of particles at the highest energies, suggesting that the steepening of the spectrum is influenced by both the GZK effect and the maximum energy achievable in extra-galactic sources. [18]

When primary cosmic rays interact with the particles present in the interstellar medium (ISM), the process known as spallation occurs. Spallation refers to the fragmentation of the primary cosmic rays, leading to the production of secondary cosmic ray particles. These secondary particles can include protons, neutrons, electrons, positrons, and various types of nuclei.

2.1.2 Cosmic ray accelerators

Finding the precise sources of cosmic rays has been a longstanding challenge owing to alterations to their paths as they encounter turbulent magnetic fields between their source and Earth. The observed cosmic ray spectrum suggests the presence of efficient accelerators, however, such that identifying potential acceleration mechanisms could guide us to the potential sources of cosmic rays.

In the context of cosmic ray acceleration, we can categorize potential sources into two broad classes: Galactic and extragalactic accelerators. Galactic accelerators primarily include supernova remnants (SNRs), which are con-

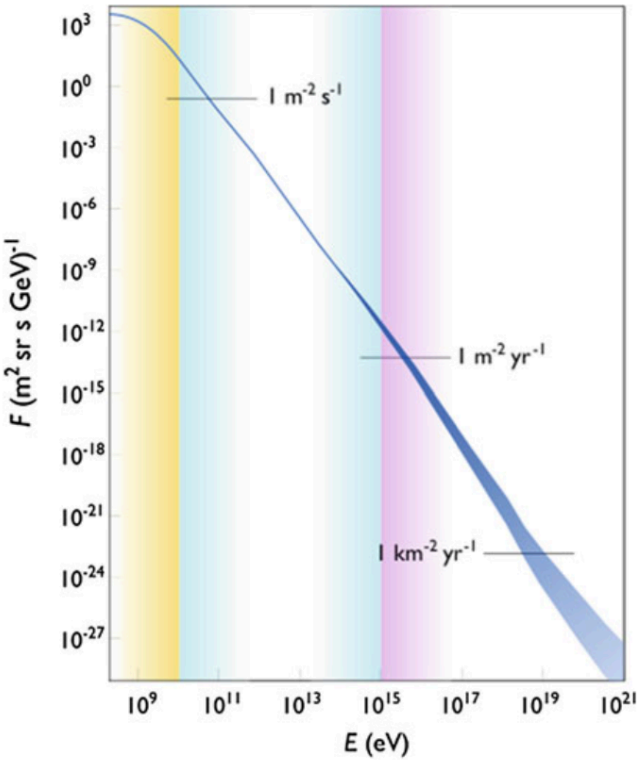

Figure 2.4: Energy spectrum of the primary cosmic rays. The vertical band on the left indicates the energy region in which the emission from the Sun is thought to be dominant; the central band represents the region in which most of the emission is presumably of galactic origin; the band on the right that of extra-galactic origin. (De Angelis & Pimenta, Introduction to Particle and Astroparticle Physics, 2018)

sidered prime sites for cosmic ray acceleration due to the strong shock waves generated during supernova events. These shock waves can efficiently accelerate charged particles to high energies through a process known as diffusive shock acceleration [19].

On the other hand, extragalactic sources of cosmic ray acceleration involve active galactic nuclei (AGNs) and gamma-ray bursts (GRBs). AGNs are powered by supermassive black holes at the centers of galaxies and are known to produce intense relativistic jets capable of accelerating particles to extremely high energies [20]. GRBs, often associated with the collapse of massive stars, release a tremendous amount of energy in a short period of time, potentially producing relativistic shock waves that can accelerate particles to ultra-high energies [21].

2.2 Multi-messenger astronomy

Traditionally, astronomy has relied heavily on the study of electromagnetic radiation across various wavelengths, from radio waves to gamma rays. However, electromagnetic radiation alone provides only a partial view of the

universe. In addition to electromagnetic waves, we can observe cosmic rays, neutrinos, gravitational waves, and other elusive particles or phenomena. Each of these cosmic messengers carries unique information about astrophysical processes and sources, providing complementary insights into the nature and dynamics of the universe. Multi-messenger astronomy is a rapidly evolving field of research that aims to study the universe using multiple cosmic messengers. By analyzing and interpreting data from different messengers, scientists might glean new insights into cosmic ray origins.

In a significant milestone for multi-messenger astronomy, a gravitational wave signal from a merging binary neutron star system was found to be accompanied by a burst of gamma rays [22]. The observation of the gravitational wave event, along with the associated gamma-ray burst, provides compelling evidence for the connection between gravitational waves and gamma-ray bursts.

Furthermore, the IceCube Neutrino Observatory detected neutrino emissions from the direction of the blazar TXS 0506+056 [23]. The correlation between the detected neutrinos and the gamma-ray emissions from the blazar provides a compelling indication of high-energy astrophysical processes. These discoveries highlight the importance of multi-messenger approaches in advancing our understanding of the universe.

2.3 PP INTERACTION

In the pursuit of uncovering the origins of cosmic rays, the Galactic plane offers a highly promising and dynamic environment for investigating the nature and mechanisms of particle acceleration. Galactic cosmic ray accelerators are generally believed to be responsible for producing cosmic rays up to the "knee" (around 3 PeV) in the cosmic ray spectrum. SNRs and pulsars are widely recognized as the most favorable Galactic objects for producing cosmic rays of energies around PeV levels [24]. However, directly observing cosmic rays in the Galactic plane is challenging due to their deflection by magnetic fields. As Cosmic ray propagate through the universe, they produce neutrinos and gamma rays. Therefore, neutrinos and gamma rays are excellent tracers for studying cosmic rays.

When exploring the connection between high energy neutrino and gamma ray emission, proton-proton interaction is highly salient. This interaction gives rise to the production of charged and neutral pions. When these pions decay, there is simultaneous generation of high-energy neutrinos and gamma rays, which retain approximately 5 % and 10 % respectively of the energy from the primary cosmic ray [25]. (See Figure 2.5)

Therefore, in the context of gamma rays produced through hadronic interactions, it is expected that high-energy neutrinos should be inevitably generated and reach Earth simultaneously. This simultaneous production of both gamma rays and neutrinos opens up exciting possibilities for multi-messenger searches aimed at uncovering the origins of very high-energy cosmic rays [26].

Moreover, detection of gamma rays sources alone cannot reveal whether they are produced in hadronic processes. This is because astrophysical processes can produce gamma rays through alternative mechanisms, such

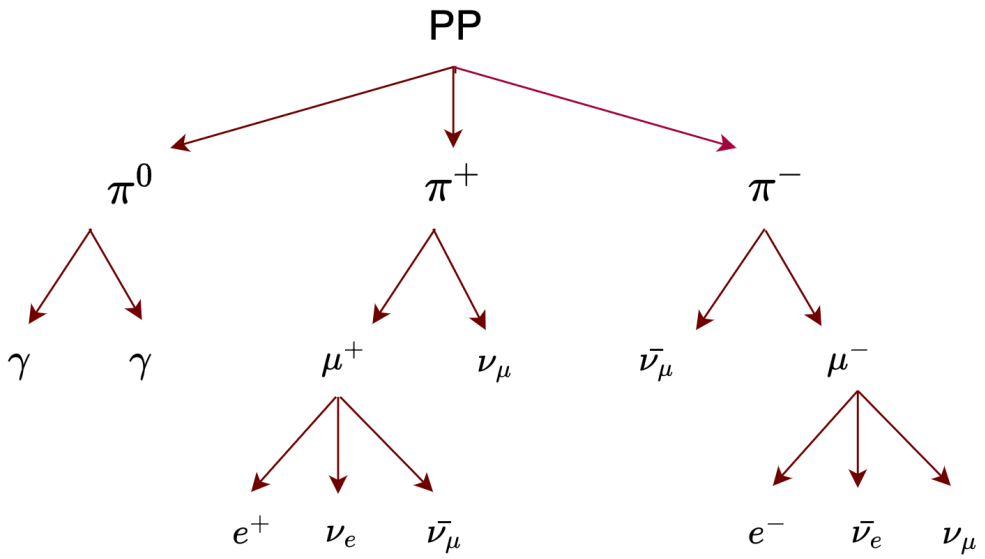

Figure 2.5: Diagram for p-p interaction

as Inverse Compton scattering and bremsstrahlung. The presence of neutrinos, however, serves as compelling evidence for the existence of their hadronic origin [27].

2.4 Neutrinos

In the context of multimessenger astronomy, where various cosmic messengers provide crucial insights into astrophysical phenomena, neutrinos are the focus of this work. In the following section, we will delve into the discovery, properties, and detection of neutrinos.

Before 1930, an issue arose in the field of nuclear physics with regard to a particular type of nuclear decay known as beta decay. This process appeared to lose energy, contradicting the conservation of energy. Wolfgang Pauli proposed a revolutionary idea that an unknown lightweight, spin 1/2 particle was being produced in beta decay, carrying away the missing energy. Initially, Pauli referred to this hypothetical particle as the "neutron," but it was later renamed as the neutrino. Neutrinos were first observed experimentally in 1956 by Clyde Cowan and Frederick Reines, who detected neutrinos produced in a nuclear reactor. The first evidence for a neutrino emission from an astrophysical source was found in 2017 through a multi-messenger observation, revealing a blazar as a source of a neutrino with energies ~ 300 TeV [23].

Neutrinos have several unique properties that make them particularly valuable for studying the universe. Unlike charged particles such as protons and electrons, neutrinos are not deflected by magnetic fields, allowing them to travel long distances without being influenced by galactic and extra-galactic magnetic fields. Neutrinos come in three flavors, electron, muon, and tau, and oscillate between these flavors as they travel through space.

2.4.1 Neutrino Detection

The most widely exploited technique of detecting cosmic neutrinos is through the fascinating phenomenon wherein charged particles, generated from interactions between neutrinos and a transparent medium, water or ice, emit Cherenkov radiation when they exceed the speed of light in that medium[28]. Due to the small cross-section of neutrino interactions and the low flux of astrophysical neutrinos expected to reach Earth, it is crucial to have a large detection volume [29].

In order to capture the Cherenkov photons emitted by swiftly moving charged particles, an array of photomultiplier tubes (PMTs) is strategically positioned within the water or ice. The arrangement of these PMTs is carefully designed to maximize the efficiency of photon detection [29]. The position of the events, along with their precise arrival times and their charge, provides essential information to construct their energy and direction.

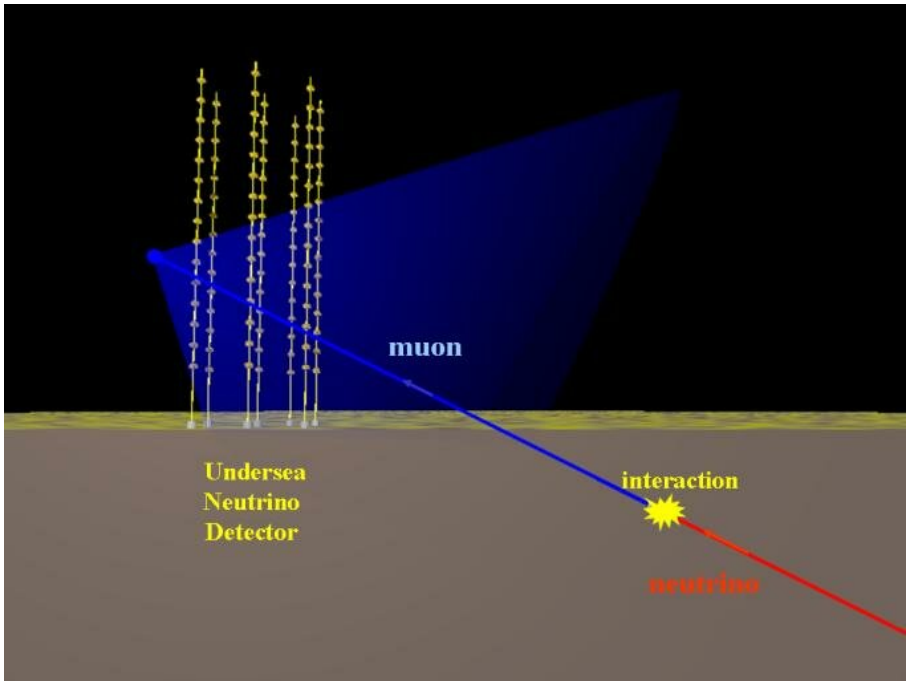

Figure 2.6: Principle of detection of high energy neutrinos in an underwater neutrino telescope. Adopted from [3]

In a neutrino telescope, backgrounds only arise from two sources: muons or neutrinos produced from cosmic ray interactions in the Earth's atmosphere. These muons, known as "atmospheric muons," can penetrate the water above the detector and contribute to a reducible background. On the contrary, neutrinos, referred to as "atmospheric neutrinos," constitute an irreducible background [**?**]. Below is a concise overview of how some of the neutrino experiments operate.

In neutrino telescopes, two main event topologies can be distinguished: tracks and showers. These events arise from different types of neutrino interaction within the detector medium.

Muon neutrinos and anti-neutrinos participate in charged current (CC) interactions, resulting in the produc-

tion of relativistic muons. These muons can travel significant distances through the detector medium, emitting Cherenkov light along their path. As a result, CC interactions leave a distinctive track-like signature in the detector. On the other hand, both neutral current (NC) interactions and CC interactions involving electron and tau neutrinos and antineutrinos produce shower-like events. In these events, the emission of Cherenkov light is nearly spherically symmetric around the shower maximum.

The track topology, provided by the muon's trajectory, offers advantages in terms of reconstructing the particle direction. This leads to a higher median angular resolution, making tracks particularly suitable in the search for point-like sources of neutrinos. On the other hand, showers offer advantages in terms of energy reconstruction, as the topology allows for a calorimetric measurement of the particle's energy. [29]

2.4.2 ANTARES

The ANTARES neutrino detector is situated in the Mediterranean Sea, 40 km south of Toulon, France. Completed on 29 May 2008, it is the largest neutrino telescope in the northern hemisphere, and the first to operate in the deep sea [30]. The detector consists of 885 optical modules (OMs), each housing a 10" PMTs oriented at a 45 degree downward angle to maximize the detection of Cherenkov photons from up-going charged particles (those produced by neutrinos that travelled through the Earth). The OMs are arranged in a three-dimensional array along 12 vertical lines spaced 60-75 m apart, with a total instrumented volume of approximately 0.01 km^3. (See Figure 2.7)

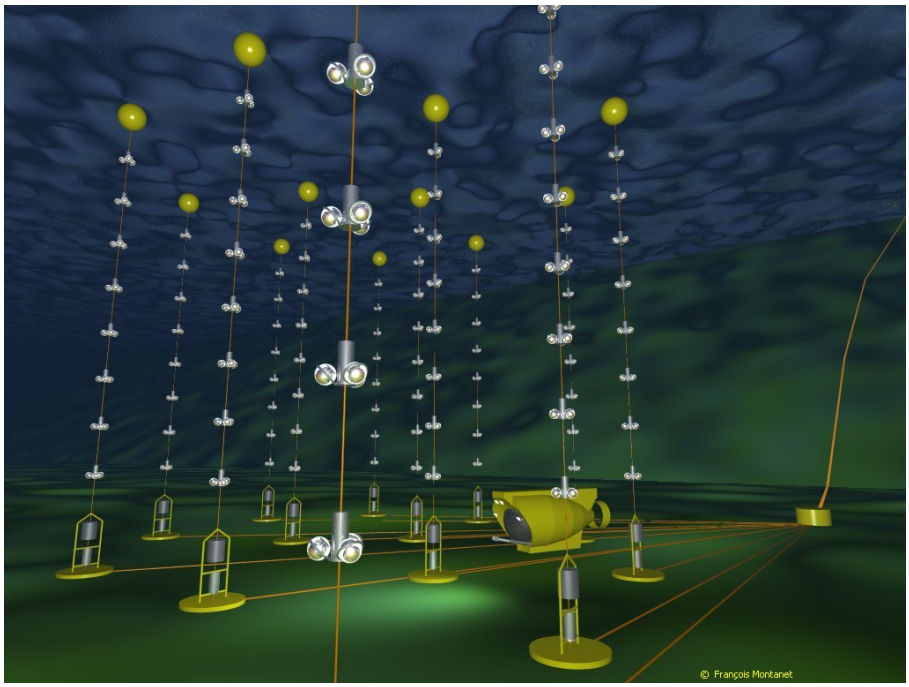

Figure 2.7: Artistic view of ANTARES telescope. Adopted from [3].

2.4.3 IceCube

The IceCube telescope is located at the South Pole and has a cubic-kilometer-sized detector that extends between 1450 and 2450 m below the surface of the Antarctic ice [28]. The South Pole ice cap, which is about three kilometers thick, provides a large quantity of interaction material and a medium of excellent optical qualities, making it an ideal location for the telescope. The detector comprises 5160 digital optical modules (DOMs), each consisting of a 10 PMTs facing downward [28]. These modules are attached to 86 vertical strings, spaced at a mean distance of ~125 m. The construction of the IceCube detector began in 2005 and was completed six years later (see Figure 2.8).

Figure 2.8: IceCube Neutrino Observatory at the South Pole in 2023 by Christopher Michel.

2.4.4 KM3NeT

The KM3NeT collaboration [31] is currently engaged in developing a future network of neutrino telescopes in the Mediterranean Sea with an anticipated instrumented volume of approximately one cubic kilometer. It comprises two detectors, KM3NeT/ARCA and KM3NeT/ORCA, which both employ the same technology but have distinct physics objectives [32][33].

KM3NeT/ARCA, located near the Sicilian coast, aims to study high-energy neutrinos from astrophysical sources. On the other hand, KM3NeT/ORCA situated off the coast of Toulon, focuses on studying atmospheric

neutrinos. Both detectors detect neutrinos by measuring the Cherenkov light produced from neutrino interactions in the seawater. This is achieved through a network of DOMs housing PMTs and their associated electronics. The DOMs are arranged on vertical string structures called Detection Units (DUs), anchored to the seafloor, and kept vertical by buoyancy.

KM3NeT/ARCA consists of two building blocks, each containing 115 DUs with 18 DOMs per string. The average horizontal spacing between strings is approximately 90 meters, while the vertical spacing is around 36 meters. In contrast, KM3NeT/ORCA consists of a single block with an average horizontal spacing of approximately 20 meters and a vertical spacing of about 9 meters. The instrumented volume is approximately 1 cubic kilometer for KM3NeT/ARCA and 7×10^6 cubic meters for KM3NeT/ORCA, making KM3NeT/ARCA more suitable for studying TeV-PeV energy range phenomena and KM3NeT/ORCA for the GeV energy range.

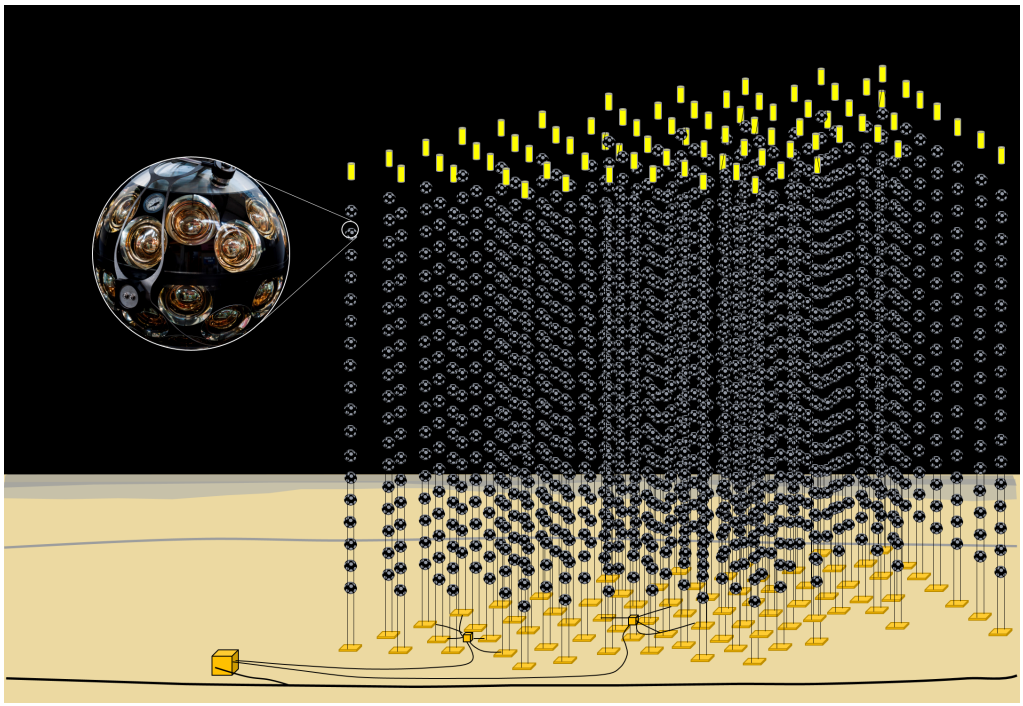

Figure 2.9: Impression of the KM3NeT detector with the multi-PMT optical module. Taken from KM3NeT Collaboration Website, https://www.km3net.org

2.5 Gamma rays

Gamma rays are a form of high-energy electromagnetic radiation with photon energies typically ranging from a few hundred keV up to TeV energies and beyond. Gamma rays possess unique properties that make them important tools for studying the high-energy universe. They are highly penetrating and can traverse vast distances without being significantly absorbed or deflected by intervening matter. Using the latest instruments, researchers

have successfully identified many gamma-ray sources inside and outside of our galaxy. Gamma rays can be generated through different mechanisms, including both leptonic and hadronic processes. The astrophysical candidates that can produce VHE gamma rays are pulsar wind nebulae, supernova remnants, and binary systems.

Gamma-ray detection is typically achieved using imaging atmospheric Cherenkov telescopes such as H.E.S.S or space-based instruments, such as the Fermi Gamma-ray Space Telescope [34]. When high-energy gamma rays interact with the Earth's atmosphere, they initiate a cascade of secondary particles, resulting in an atmospheric phenomenon known as an air shower. Within these air showers, charged particles emit Cherenkov radiation as they move through the atmosphere. H.E.S.S, located in Namibia, is specifically designed to Cherenkov radiation generated by the charged particles within the air shower within the energy range of 20 GeV to 100 TeV.

H.E.S.S consists of four identical telescopes with mirrors of 12 m diameter each and a fifth telescope with a mirror of 28 m diameter (See Figure 2.10). This telescope array is instrumental in the H.E.S.S Galactic Plane Survey, which will be discussed in more detail later in this thesis.

Figure 2.10: View of the full H.E.S.S. array with the four 12 m telescopes and the 28 m H.E.S.S. II telescope in Namibia (image credit: H.E.S.S. Collaboration, Clementina Medina)

3

Simulating Galactic Neutrino Sources

In our study, we use Galactic gamma ray sources to predict neutrino emissions. The connection between gamma rays and neutrinos arises from the production of both particles in high-energy hadronic interactions.

In this chapter, we present a methodology to estimate overall emission of neutrinos from the Milky Way stemming from sources. We begin by providing an overview of the foundation on which our model is built, drawing inspiration from the work of Batzofin and Komin [1]. Their research serves as a crucial starting point for our investigation and, using their results, we develop a model to quantify the relationship between neutrino and gamma ray fluxes, ultimately paving the way for improved predictions of neutrino emissions. To carry out our analysis, we utilize synthetic populations of VHE gamma-ray sources, obtained from [35]. Taking this dataset, we apply our model to predict the corresponding neutrino emissions associated with these gamma-ray sources. Additionally, we make use of the Python Gammapy package to generate skymaps, which offer a visual representation of the spatial distribution of the predicted sources across the galactic plane as well as their fluxes. Furthermore, we analyse the accuracy of our model by comparing it with observed neutrino events recorded by neutrino telescopes.

3.1 Correlating gamma ray and neutrino fluxes

The study was based on the work of Batzofin and Komin, titled "Predicting Neutrino Emission for the Sources in the H.E.S.S. Galactic Plane Survey" [1], which aimed to make accurate calculation of the neutrino flux from sources in the H.E.S.S. Galactic plane survey [36].

The sources detected by H.E.S.S. can be categorized into four different groups based on their potential origin: SNRs, binary systems, pulsar wind nebulae (PWNe), and unidentified sources. The authors of the paper [1] developed a method for predicting possible neutrino emission from the H.E.S.S. Galactic plane survey. They used

a parameterization of the proton spectrum for each source based on the model of Kelner et al [37] and Naima [38].

The Kelner model [37] is a parametrisation of the cross section determined from simulations, which is then used to derive the spectrum of secondary particles like gamma-rays or neutrinos produced in proton-proton collisions in the very high energy regime. The Naima package [38] is a Python software package that provides a toolkit for modeling astrophysical non-thermal radiation from relativistic particle populations and is widely used in the field of high-energy astrophysics. Specifically, for each of the sources in the H.E.S.S. Galactic Plane Survey, they first obtained the proton spectrum, by implementing Naima and the Kelner model, and used this proton spectrum to predict the neutrino flux. The result of their study is shown in Figure 3.1.

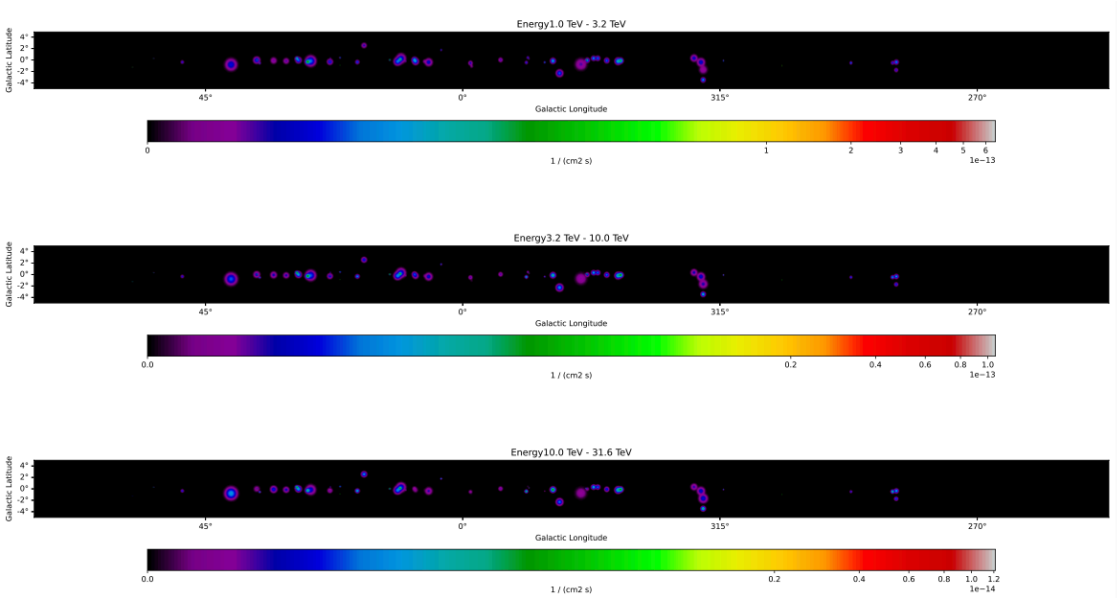

Figure 3.1: Predicted integrated neutrino flux map of the Milky Way for different energy bins. (Batzofin and Komin, 2021)

To simplify the process of predicting neutrino emissions from very-high-energy gamma-ray sources, we established a conversion function, denoted as 'f(E),' that correlates gamma-ray spectra into neutrino spectra. We utilized the results obtained by Batzofin et al. [1] to derive this conversion function. Instead of directly calculating neutrino fluxes using the Kelner parametrisation [37], we opted for a more efficient approach. We divided the predicted neutrino fluxes, as determined by Batzofin et al., by the observed H.E.S.S. gamma-ray fluxes for each source. These ratios were averaged over all sources, which allowed us to create a more representative conversion function over the energy range of 0.1 to 100 TeV. This function is depicted in Figure 3.2. By fitting this conversion function using Python, we established a correlation between the gamma-ray spectrum and the neutrino spectrum. This correlation facilitates the direct estimation of the neutrino flux based on a given gamma-ray flux, obviating the need for detailed proton distribution calculations using Naima and Kelner parametrisation. Namely, the neutrino flux

corresponding to a given gamma ray flux can be computed with:

$$\frac{dN_\nu}{dE_\nu} \approx f(E) \times \frac{dN_\gamma}{dE_\gamma} \tag{3.1}$$

where $f(E)$ is the function we aim to find, which co-relates neutrino differential flux ($\frac{dN_\nu}{dE_\nu}$) to gamma ray fluxes ($\frac{dN_\gamma}{dE_\gamma}$).

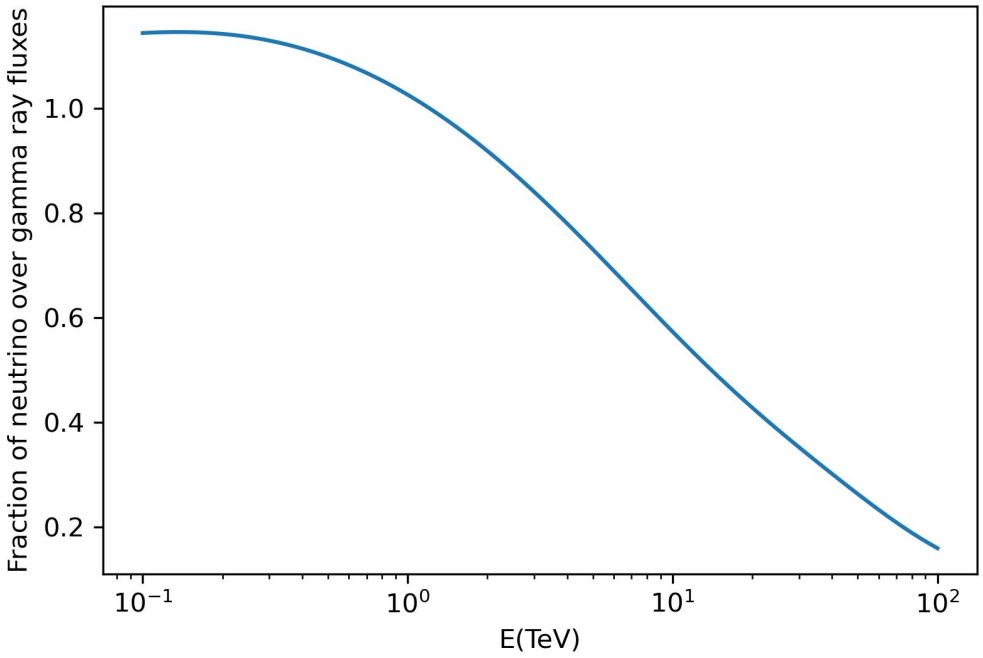

Figure 3.2: Fraction of Batzofin et al. (2019) predicted neutrino fluxes over the observed H.E.S.S. gamma ray

The fitted function, describing the fraction shown in figure 3.2, is then found through Python as:

$$f(E) = \frac{a}{\sqrt{b(E-c)}} + d \tag{3.2}$$

Where E is the energy and the constants are:

$$a \simeq 1.67 \times 10^{2}$$
$$b \simeq 1.42 \times 10^{4}$$
$$c \simeq -3.00$$
$$d \simeq -4.84 \times 10^{-2}$$

It is important to note that, in this modeling of the predicted neutrino spectra, several assumptions were made:

- No contribution of non-hadronic processes to the measured γ-ray signal.
- No significant γ-ray absorption within the source.
- Charged pions decay before interacting.
- Muons decay without significant energy loss.
- The neutrino flux at earth is computed by assuming the flavour ratio ($\nu_e : \nu_\mu : \nu_\tau = 1 : 1 : 1$). This is a direct consequence of neutrino oscillation [39].

As mentioned in section 2.5, in the pp interaction, ν_μ and ν_e are produced. Therefore, the total neutrino flux obtained will be a combination of both:

$$\text{Total neutrino flux in pp interaction}: \frac{dN_{\nu_{toal}}}{dE_{\nu_{total}}} = \frac{dN_{\nu_\mu}}{dE_{\nu_\mu}} + \frac{dN_{\nu_e}}{dE_{\nu_e}} \tag{3.3}$$

Note that neutrinos and antineutrinos are treated as identical here. However, since we assumed a flavor ratio of ($\nu_e : \nu_\mu : \nu_\tau = 1 : 1 : 1$), (implying equal numbers of neutrinos of all three flavors) and we are interested in detection of muon tracks with high-energy neutrino telescopes, the total muon flux is then calculated as:

$$\frac{dN_{\nu_\mu}}{dE_{\nu_\mu}} = \frac{1}{3} \times \frac{dN_{\nu_{total}}}{dE_{\nu_{total}}} \tag{3.4}$$

This method offers a simpler way of predicting muon neutrino emissions from VHE gamma ray sources, which could facilitate the study of these sources and their physical properties. It also has the advantage of being computationally faster than the approach used by Batzofin and Komin.

To validate the accuracy and validity of our proposed model, we performed a comparison between the expected neutrino flux derived from our model and the model developed by Batzofin et al. (2019). This comparison involved applying both parameterizations to the observed H.E.S.S. sources, allowing us to assess the differences in the predicted neutrino spectra between the two models (refer to Figure 3.3 for an example of this comparison). Notably, the results of this comparison demonstrated a high level of agreement between the two models, thereby supporting the accuracy of our proposed model. It's noteworthy that the derived spectra exhibit clear deviations from the constant fraction between gamma-rays and neutrinos, which is occasionally assumed in the literature.

3.2 Gamma ray sources

In our study, we employed a synthetic population of 3000 VHE gamma-ray sources obtained from the source provided by [35]. This population consists of 831 sources, with 78 corresponding to observed sources from the H.E.S.S. Galatic Plane Survey (HGPS) [36], and the remainder simulated. The modeling of these sources adopted a 4-arm spiral structure, with each source characterized by Galactic coordinates, circular extent, distance, luminosity, radius, and integrated flux. The energy spectrum of these sources was assumed to follow a power-law model with a spectral index of 2.3, covering an energy range from 1 to 100 TeV. The following subsection outlines the construction of these synthetic populations.

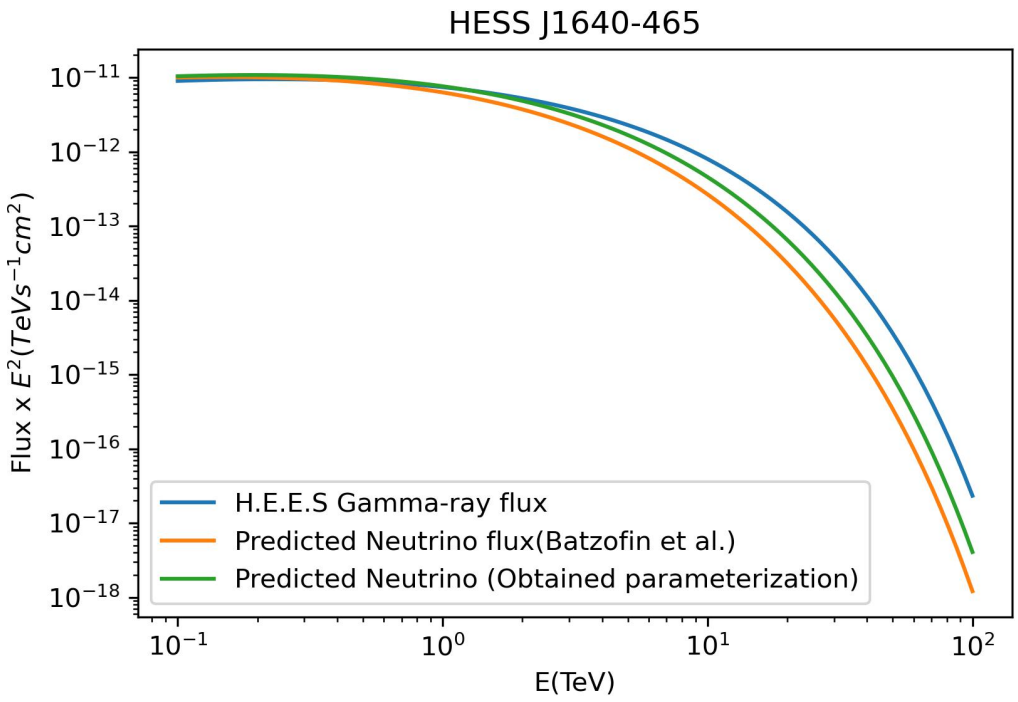

Figure 3.3: Comparing the calculated neutrino flux of our new parameterization with Batzofin et al model for one of the H.E.S.S sources

3.2.1 Construction of simulated γ-ray sources

The authors Steppa and Egberts set out to model the population of very high-energy gamma ray sources in the Milky Way galaxy in their study [35]. To achieve this, they took observational data obtained from the H.E.S.S. instrument and employed the Monte Carlo method to generate a large number of synthetic sources. By doing so, they were able to make predictions about the overall population of VHE gamma ray sources in our galaxy. Their model constituted two key components: the spatial distribution of the sources and the distribution of their properties; luminosity and radius [35].

3.2.2 Spatial model

In order to investigate the spatial distribution of VHE gamma ray sources in the Milky Way galaxy, the researchers undertook analysis involving various models based on the assumed source class and underlying Galactic structure. They then followed a data-driven approach to derive the distribution of the properties.

Since a significant proportion of the known sources are SNRs and PWNe, they employed these as templates for constructing their models. In addition to utilizing the distribution of SNRs and PWNe as templates, the

researchers explored various other models to account for distribution of gamma ray sources, namely the mSp4 model characterised by a four-arm spiral distribution (see Figure 3.4).

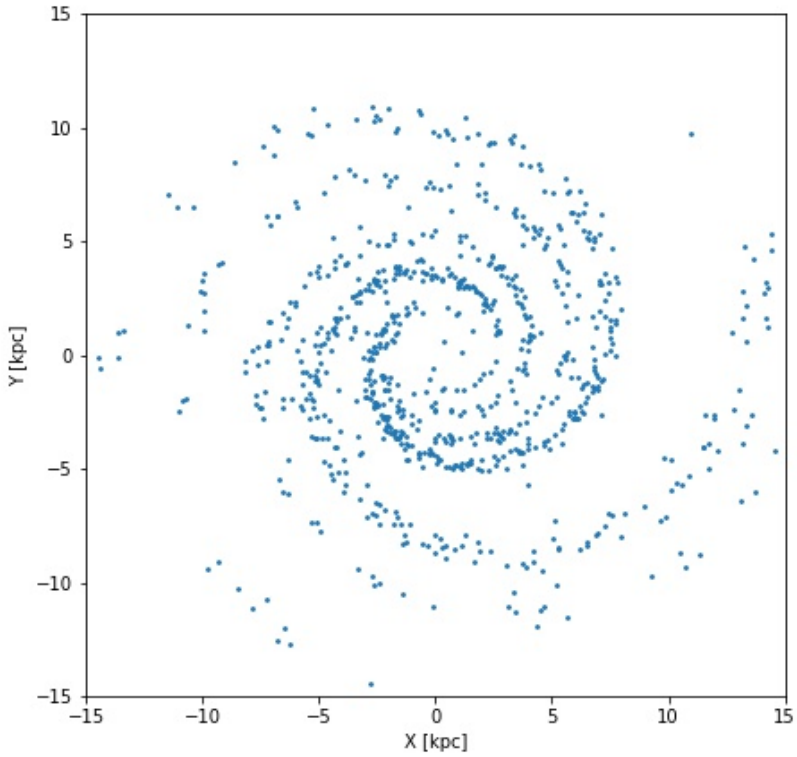

Figure 3.4: Spatial distribution of the gamma ray sources used in this research, describing the four-arms spiral model in the Galactic plane at z=0 kpc.

This model explicitly incorporates the azimuthal angle (φ) as a critical factor in determining the source density. The mathematical representation for this model is described by equation 3.5, which considers various parameters including r (radius), z (vertical coordinate), and constants such as A_i, δ, β_i, and a_i. The radial dependence is determined by the scale length σ_r and exhibits a local maximum at R, while the azimuthal dependence is influenced by the scale length δ, pitch angle constants β_i, and orientation factors a_i. Additionally, the vertical dependence is governed by the scale height $\sigma_{z,2}$.

$$\rho(r,\varphi,z) = \sum_{i_1}^{4} A_i \exp\left(\frac{-1^2}{\delta}\right)\left(\varphi - \frac{\ln\left(\frac{r}{a_i}\right)}{\beta_i}\right)^2 \times \exp\left(-\frac{r-R}{\sigma_r}\right)\exp\left(-\frac{z^2}{2\sigma_{z,2}}\right) \tag{3.5}$$

For the determination of appropriate parameter values, the researchers adopted the best-fit values derived from the Interstellar Medium (ISM) measurements associated with the CII cooling lines, as provided by Steiman-

Cameron et al. (2010).

3.2.3 Luminosity and radius distribution

Having obtained a spatial model for the distribution of VHE gamma ray sources, the next step is computation of the distribution of their luminosity L and source radius R. To simplify the analysis, the luminosity and radius are treated as independent variables, and it is assumed that both follow a simple power-law distribution. The joint probability function for the luminosity and radius is defined as:

$$P(L, R) = N \left(\frac{L}{L_0}\right)^{\alpha_L} \left(\frac{R}{R_0}\right)^{\alpha_R} \tag{3.6}$$

In equation 3.6, L_0 and R_0 are scaling factors, and N is a normalization factor that depends on the predefined boundaries of L and R. The parameters α_R and α_L are variable parameters that are determined based on the number of detected sources $N_{\rm det}$ in the H.E.S.S. Galactic Plane Survey (HGPS). The number of detected sources $N_{\rm det}$ is related to equation 3.6 through equation below as:

$$N_{det} = N_{FOV} \int dL \int dR \;\; C(L, R) P(L, R) \tag{3.7}$$

Here, the correction function $C(L, R)$ is applied to address observation biases, ensuring that the sample comprises sources that align with the detectability criteria, thus accurately representing those sources observable according to HESS sensitivity. By incorporating this correction function, the analysis aims to compensate for any systematic biases in the observed sample of sources and obtain a more accurate representation of the underlying population. On the other hand, $N_{\rm FOV}$ represents the total number of sources that are expected to exist within the field of view (FOV). The expected number of sources is approximated via

$$N_{pred,i} = C(L_i, R_i) N_{FOV} \int dL \int dR \;\; P(L, R) \tag{3.8}$$

$N_{pred,i}$ represents the number of detectable sources for each bin I, which is characterized by a $L \times R$ space split into 0.1×0.1 bins in $\log_{10}$ scale. Finally the variables α_R, α_L and N_{FOV} are determined using the likelihood as:

$$\log L = \sum \log(P_{N_{pred,i}}(N_{true,i})) \tag{3.9}$$

where $P_{N_{pred,i}}(N_{true,i})$ represents the Poissonian distribution where $N_{true,i}$ denotes the true number of detected sources. The model parameters are obtained by maximising the likelihood function in equation 3.9 using a Monte Carlo simulation approach.

3.3 Calculating Neutrino emission

With the parameterization derived in the previous section 3.1 we will now estimate the expected neutrino flux for each of our simulated gamma ray sources. As an illustrative example, we present the results for one of our gamma ray sources (See Figure 3.5).

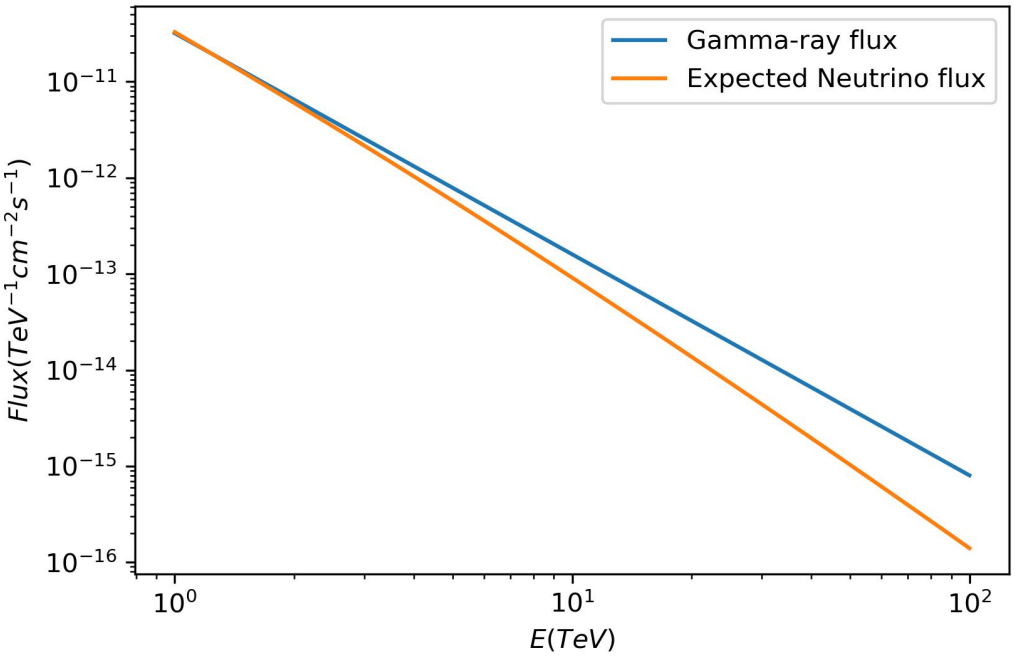

Figure 3.5: Simulated gamma ray flux and expected neutrino flux obtained for one the simulated gamma ray sources in this study.

It is important to note that the gamma ray flux follows a power-law behavior, characterized by a spectral index of 2.3. Additionally, our model (referenced as 3.1) for predicting the associated neutrino flux is valid only under the assumption of an exclusively hadronic origin for the considered gamma ray sources.

3.4 Identifying galactic neutrino sources

The model employed in this research enables us to make predictions for the neutrino emission from the Milky Way. To effectively communicate the outcomes of our investigation, skymaps were created utilizing the Python package Gammapy. Gammapy is a widely-used software toolkit specifically designed for analyzing high-energy gamma ray data and conducting astrophysical studies [40].

In the process of creating our skymaps, the Gaussian Spatial model in Gammapy was employed to represent the spatial distribution of the assumed neutrino sources within the galactic plane. The coordinates and extensions of the gamma ray sources were used as inputs to determine the positions and sizes of the corresponding assumed neutrino sources. This approach is based on the fundamental assumption that both gamma ray and neutrino emissions originate from the same astrophysical hadronic sources, thereby sharing similar spatial characteristics. In addition to spatial information, spectral considerations were incorporated into the skymap generation process.

A template spectral model was applied to each assumed neutrino source using our proposed model, enabling the calculation of the expected neutrino flux associated with each individual source.

Skymaps were generated for each gamma ray population to comprehensively analyze the potential neutrino sources. The spatial range selected for this analysis spanned 0 to 360 degrees in galactic longitude and -5 to 5 degrees in galactic latitude, effectively covering the entire galactic plane.

4

The Galactic Sky in Neutrinos

In this thesis, the simultaneous production of neutrinos and gamma rays through pp interactions helped us to develop a Parametrization that corelates gamma ray and neutrino fluxes. Subsequently, we applied this model to 3000 populations of the VHE gamma-rays sources, comprising both simulated and observed sources within the Milky Way, to predict potential galactic neutrino emissions. By using the Gammapy package in Python, we produced sky maps to visualize these predicted neutrino sources, highlighting their corresponding fluxes magnitudes and position in the sky. Figure 4.1 exhibits a truncated view of 4 different skymaps. Additionally, Figure 4.2 and Figure 4.3 display the full skymaps of two samples covering the whole galatic plane. The color intensity of the pixels indicates the flux of neutrinos associated to each source.

Using the fluxes of the sources in our model, we conducted an average of the flux from all populations to obtain the total predicted neutrino flux. This calculated flux was then compared to the diffuse flux observed by IceCube and the upper limit established by ANTARES. The comparison results, depicted in Figure 4.4, highlight the fact that our total predicted neutrino flux is expected to be lower than both the total IceCube flux and the upper limit set by ANTARES. This is because our predicted galactic neutrino sources constitute a subset of the overall neutrinos coming from both Galactic and extra-galactic sources. Our model does not accounts for all possible sources of neutrino events, but focuses specifically on those originating within our galaxy.

To validate the accuracy of our predictions, we compare our model with the data obtained from neutrino detectors. IceCube and ANTARES are two prominent experiments designed to capture neutrino events. However, their locations and detector designs result in variations in their observational capabilities. IceCube is situated at the South Pole, while ANTARES is located in the Mediterranean Sea. This geographical distinction plays a crucial role in their field of view, particularly regarding the observation of the galactic plane. It is important to note that the galactic plane is better observed in the southern sky compared to the northern sky. Figure 4.5 clearly demonstrates that ANTARES exhibits enhanced sensitivity in the southern sky [41]. This disparity arises due

to the classification of events from the Southern Sky as down-going events in the case of IceCube, a significant portion of which, prior to any selection criteria, are attributed to atmospheric muons. Conversely, ANTARES faces a different scenario when observing the southern sky, with a lower presence of atmospheric muons owing to the shielding effect of the Earth [29]. This distinction enhances the performance of ANTARES in terms of detected events related to the galactic plane, making it an ideal choice for our project.

We made a comparison between our model and eleven years of data obtained from the neutrino detector ANTARES. We utilize eleven years of ANTARES data recorded between 2007 and 2017, resulting in a total lifetime of 3136 days. This dataset [42][43] encompasses a substantial number of track-like events, totaling 8754, which are employed for comparison with our predicted results. For a better visualization of the spatial distribution of the data refer to Figure 4.6.

Since the ANTARES data covers the entire sky and our skymap focuses only on the galactic plane, we need to determine how many ANTARES data points coincide spatially with the pixels in our skymap. To facilitate the comparison, we generated a histogram that measures the spatial overlap between the ANTARES data and the pixels in the skymaps. 747 events survived these criteria.

Furthermore, to facilitate the comparison between our predicted neutrino sources and the ANTARES data, it was necessary to calculate the expected counts by our model. This involved taking into account various factors such as the neutrino flux, the effective area of the telescope (A_{eff}), and the observation time (T). The number of counts is then obtained as:

$$N_{\nu_\mu} = T \int_{E_{\min}}^{E_{\max}} \frac{dN_{\nu_\mu}}{dE_{\nu_\mu}} \, A_{\text{eff}}(E) \, dE_{\nu_\mu} \tag{4.1}$$

Where $E_{\min}$ and $E_{\max}$ are 1 and 100 TeV, and T is 27×10^7 seconds, encompassing the eleven-year data span from 2007 to 2017. The effective area of the ANTARES neutrino telescope, which represents its detection capability, is energy-dependent and also varies with the declination of the source; it is adopted from [6] presented in the figure 4.9. Finally, we repeated the same process for KM3NeT configuration 2. The only difference was the use of a different effective area, which is shown in Figure 4.8. With this information, we calculated expected counts for each source.

Using neutrino fluxes and solid angles derived from our maps, along with the effective area and observation time of the telescope, we estimated the number of expected neutrino events for each source. We found that a significant portion of the sources we predict do not yield any neutrino counts. However, for a subset of sources, we obtained a count of one neutrino. The expected count distribution for ANTARES is illustrated in Figure 4.10, as you see expect 54 counts for ANTARES in average.

It is important to note that as the rather homogeneous distribution of 747 recorded ANTARES counts suggests, most of them are likely not associated with Galactic sources, since the number overshoots the predicted counts of 54 derived from the simulations. In contrast to ANTARES predictions, 11 years of KM3NeT observations are shown to provide a much more detailed view of the Galactic sky, with several sources clearly identified

with a larger number of neutrinos from the same direction. The predicted count distribution for KM3NeT exhibits an average count of 222, as shown in Figure 4.11.

The count plot, depicted in Figure 4.13 and 4.12, illustrates the positions of the potential neutrino sources and their corresponding expected numbers of neutrinos for one of two of our samples. Each data point in the plot corresponds to a specific source, with the x-axis representing the spatial position and the y-axis indicating the expected neutrino counts. We present more plots and sky maps in the appendix.

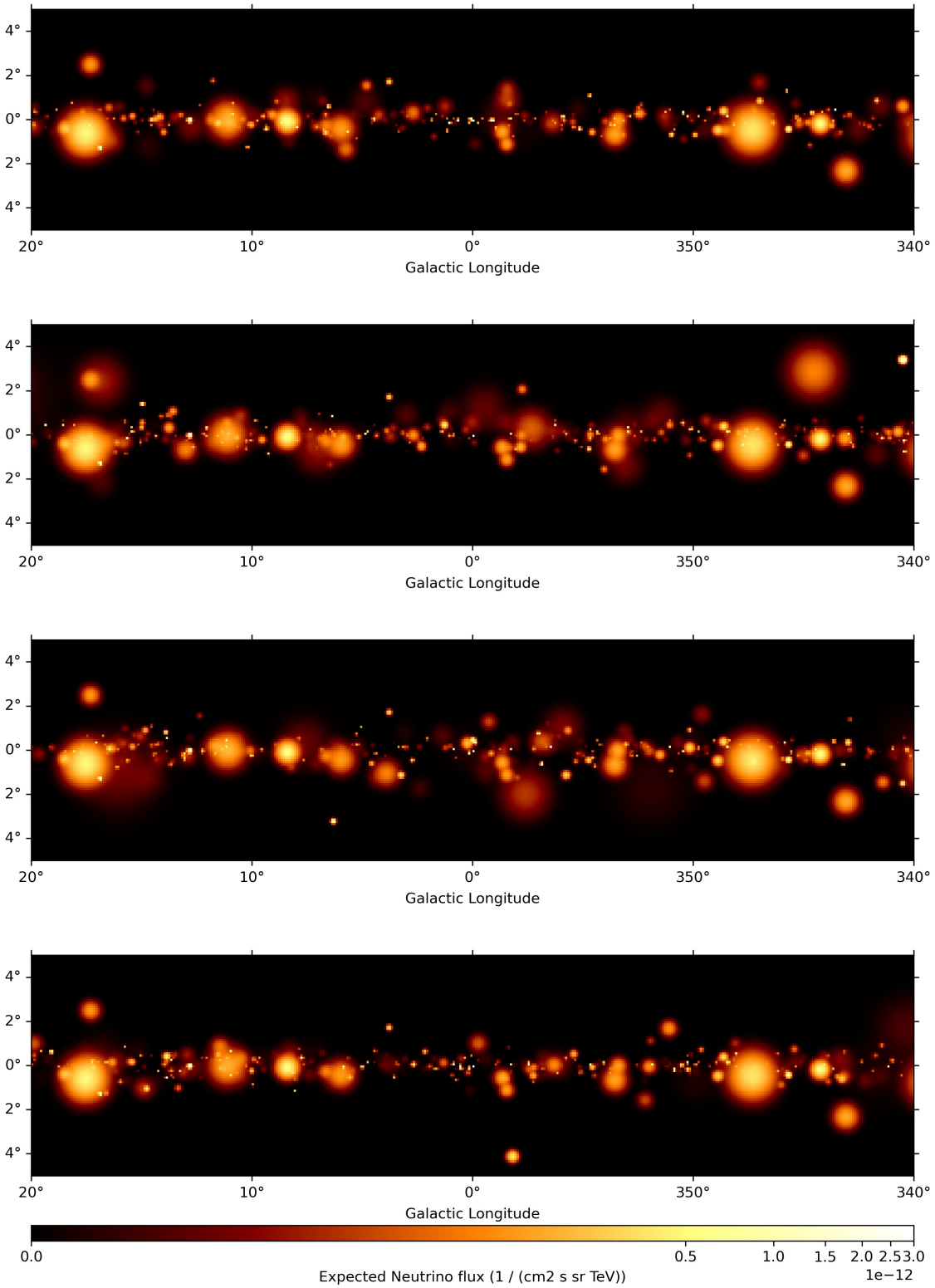

Figure 4.1: Cutout of Sky maps for 4 different samples showing neutrino sources and their flux in the energy bin of 54.6 to 57.2 TeV

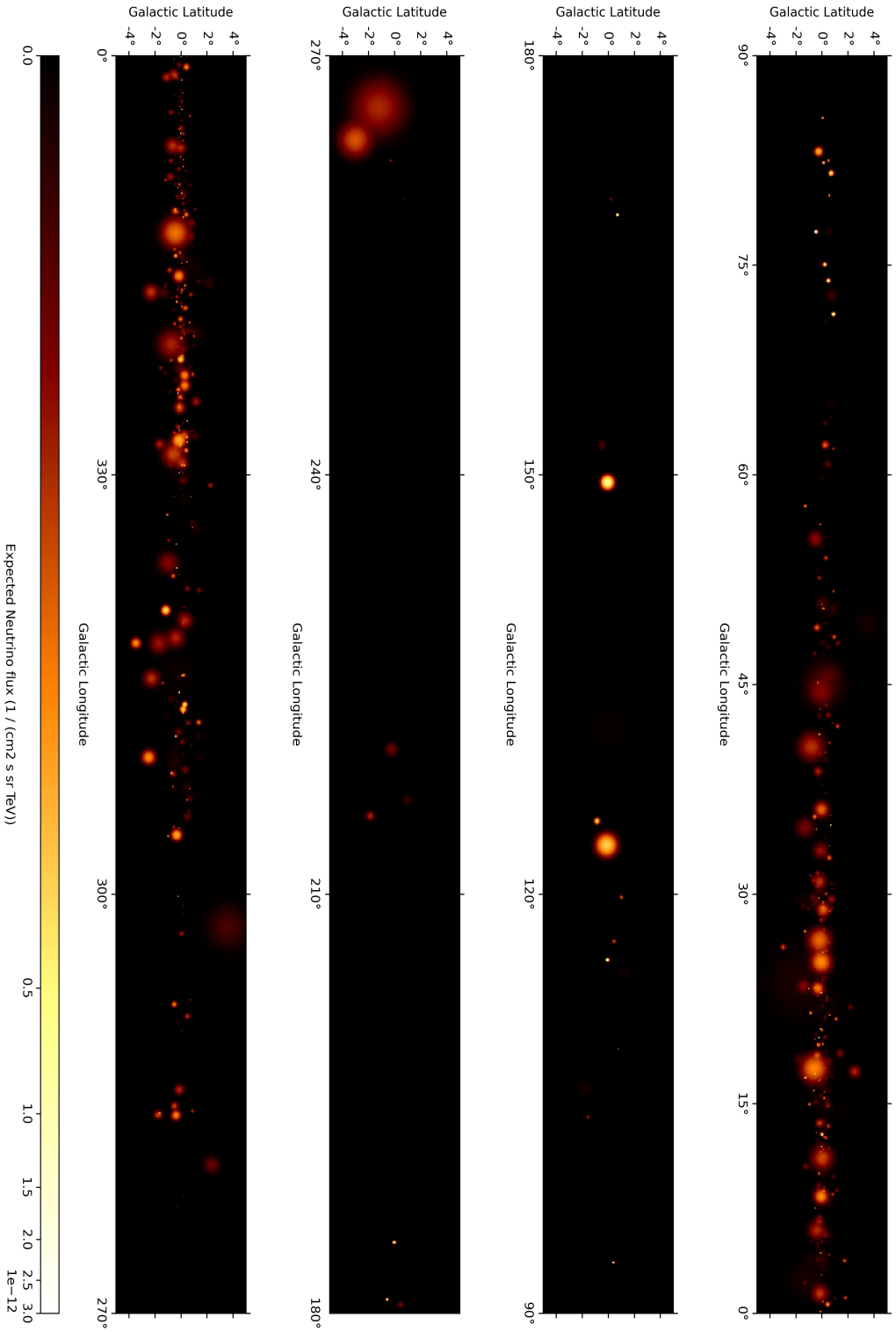

Figure 4.2: sky map for one of the samples population showing neutrino sources and their flux in the energy bin of 95.5 to 100 TeV

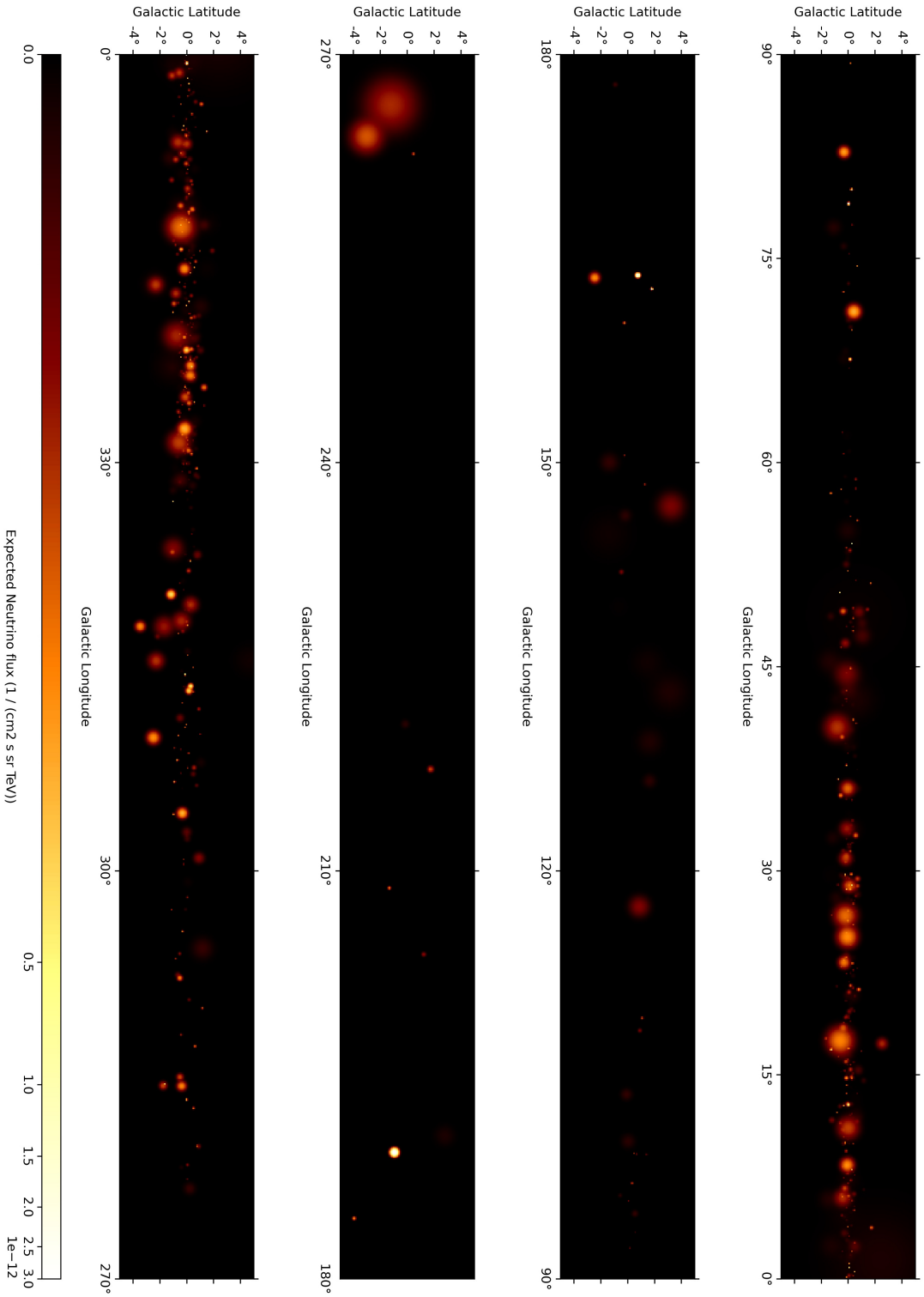

Figure 4.3: sky map for one of the samples population showing neutrino sources and their flux in the energy bin of 95.5 to 100 TeV

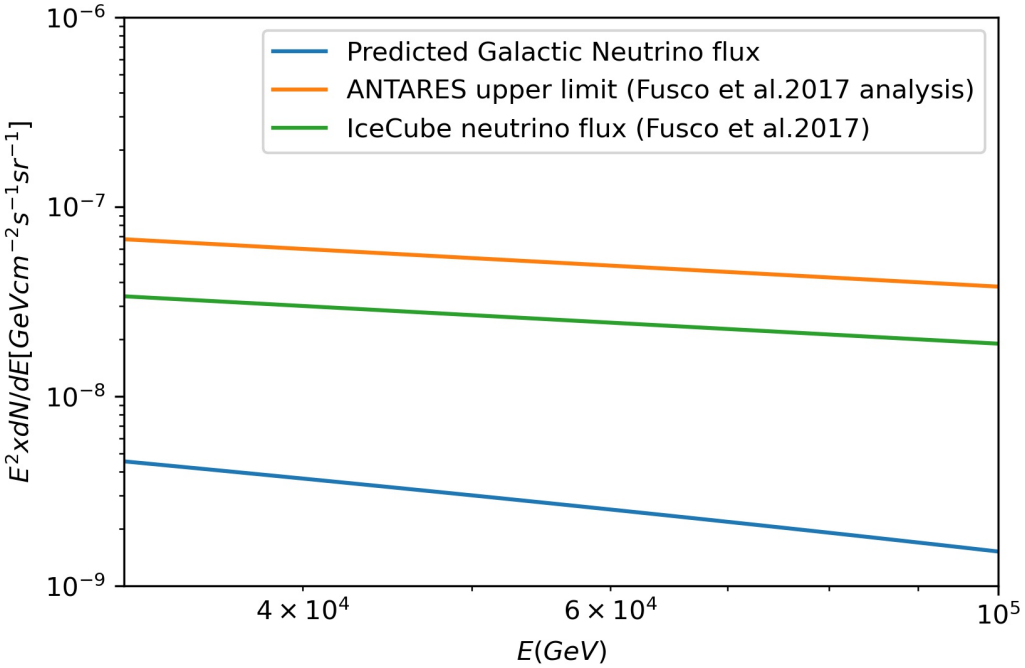

Figure 4.4: Total predicted neutrino flux compared with IceCube diffuse flux and ANTARES upper limit

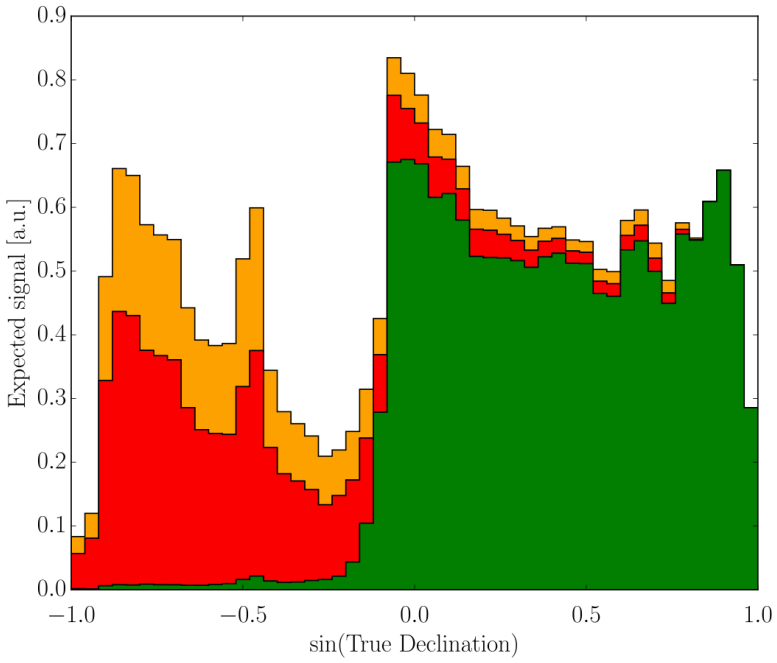

Figure 4.5: Stacked histograms (i.e., every bin shows the fractional contribution of every sample summed on top of each other) of the signal neutrino expected as function of the declination. The yellow and red colors correspond to ANTARES showers and tracks respectively. While, the green color represents IceCube tracks. (The plot is adopted from [4])

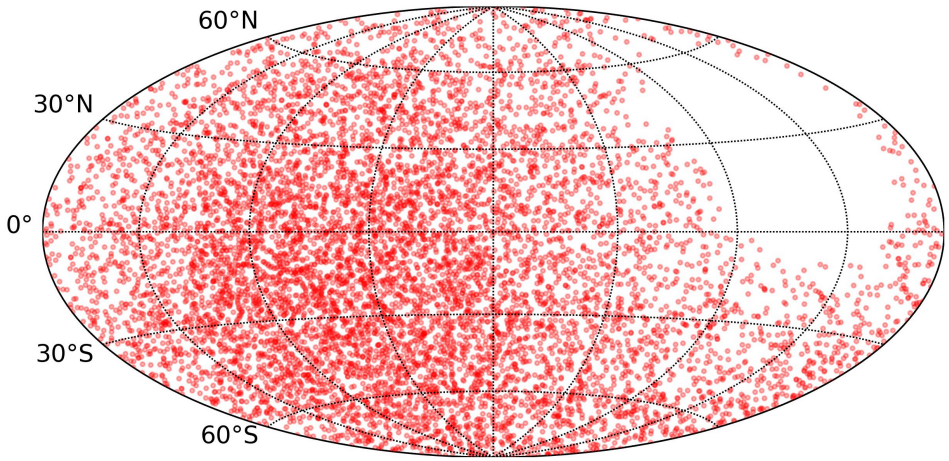

Figure 4.6: A flat projection of the observed neutrino events by ANTARES from 2007 to 2017, covering the entire sky. The meridians on the plot represent galactic longitudes, from -180 to 180 degree, while the other lines represent galactic latitudes, ranges from -90 to $+90$ degree

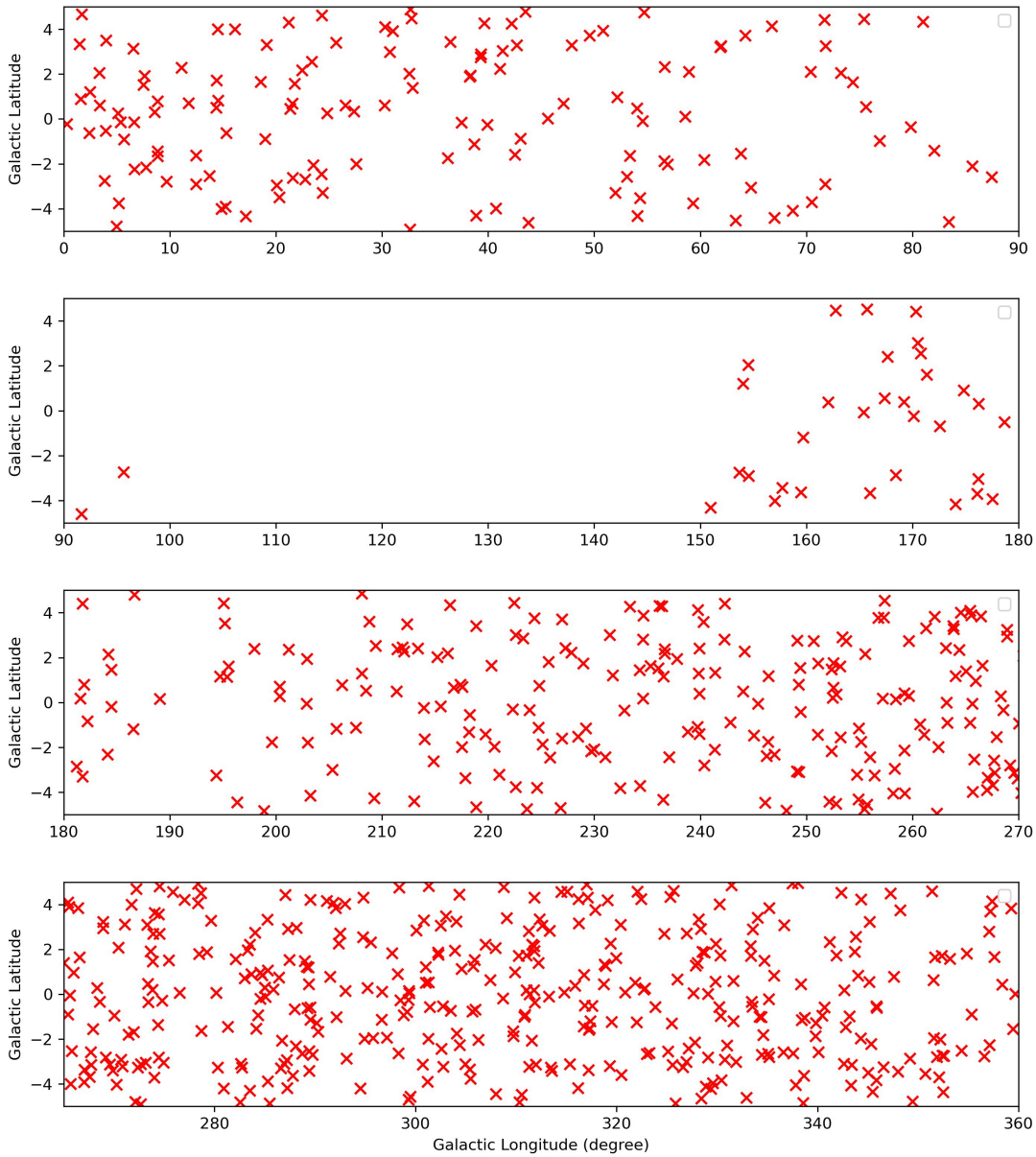

Figure 4.7: Cross points represent the observed neutrino events by ANTARES from 2007 to 2017 in the Galatic plane.

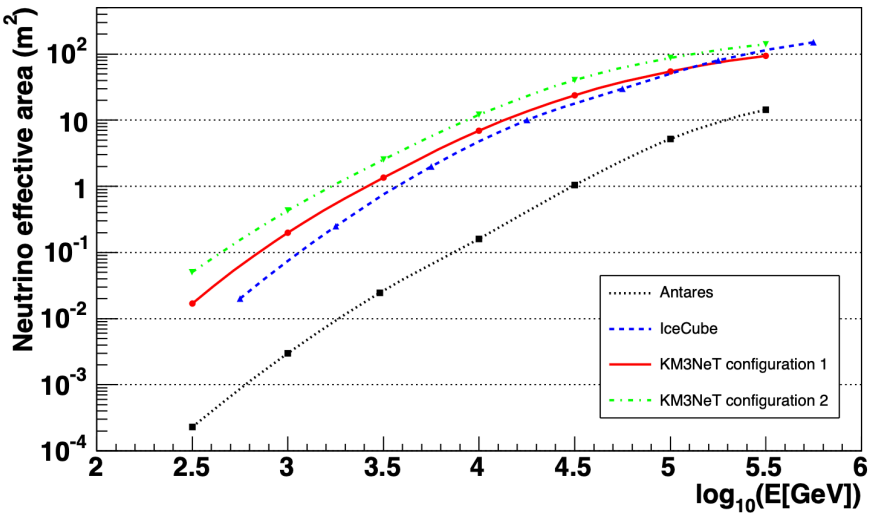

Figure 4.8: Neutrino effective areas for the considered KM3NeT configurations. The ANTARES and IceCube effective areas are shown for comparison. Adopted from [5]

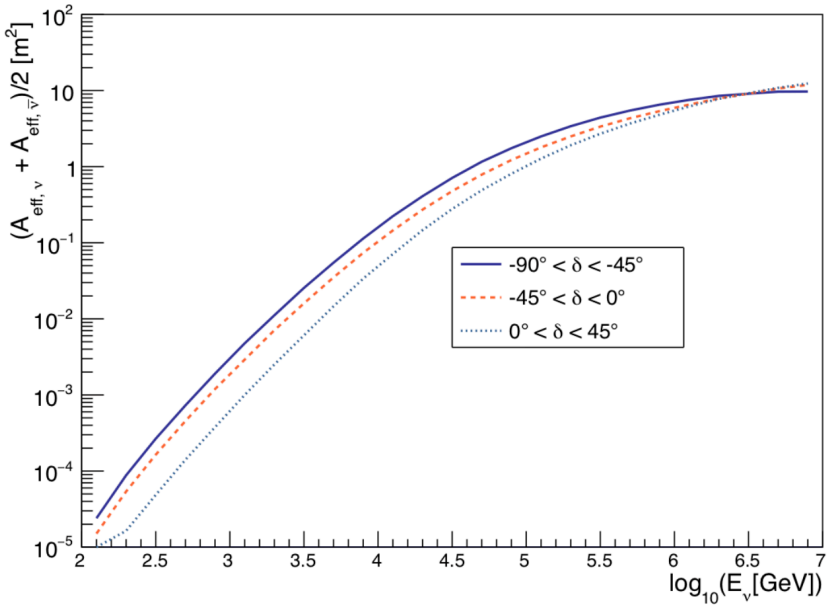

Figure 4.9: ANTARES effective area as function of energy (taken from [6])

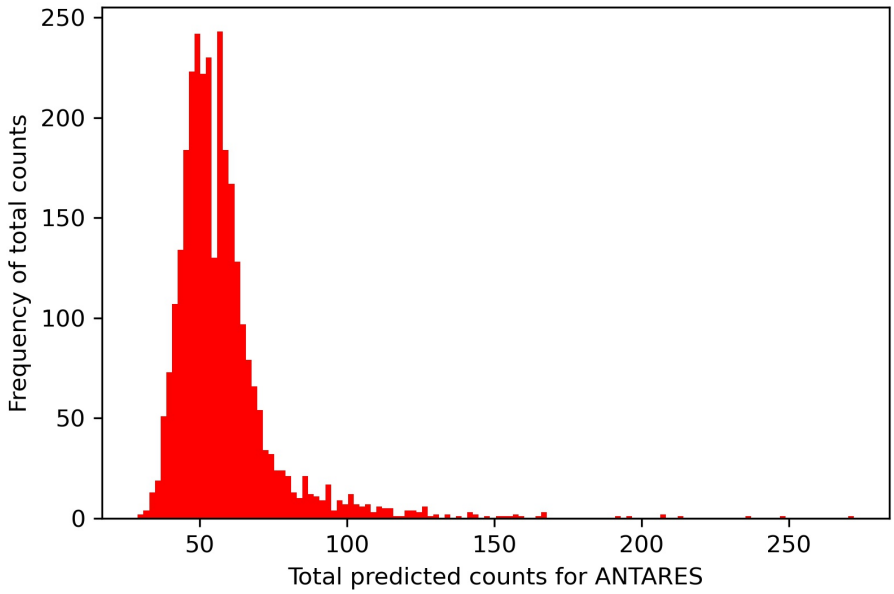

Figure 4.10: Distribution of the total expected Neutrino Counts for ANTARES for all the 3000 samples

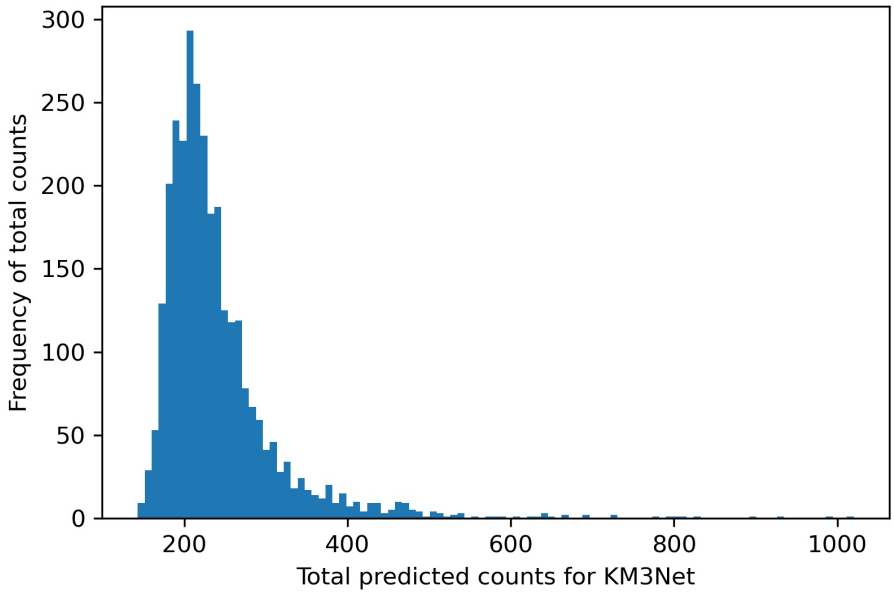

Figure 4.11: Distribution of the total predicted Neutrino Counts for KM3NeT for all the 3000 samples

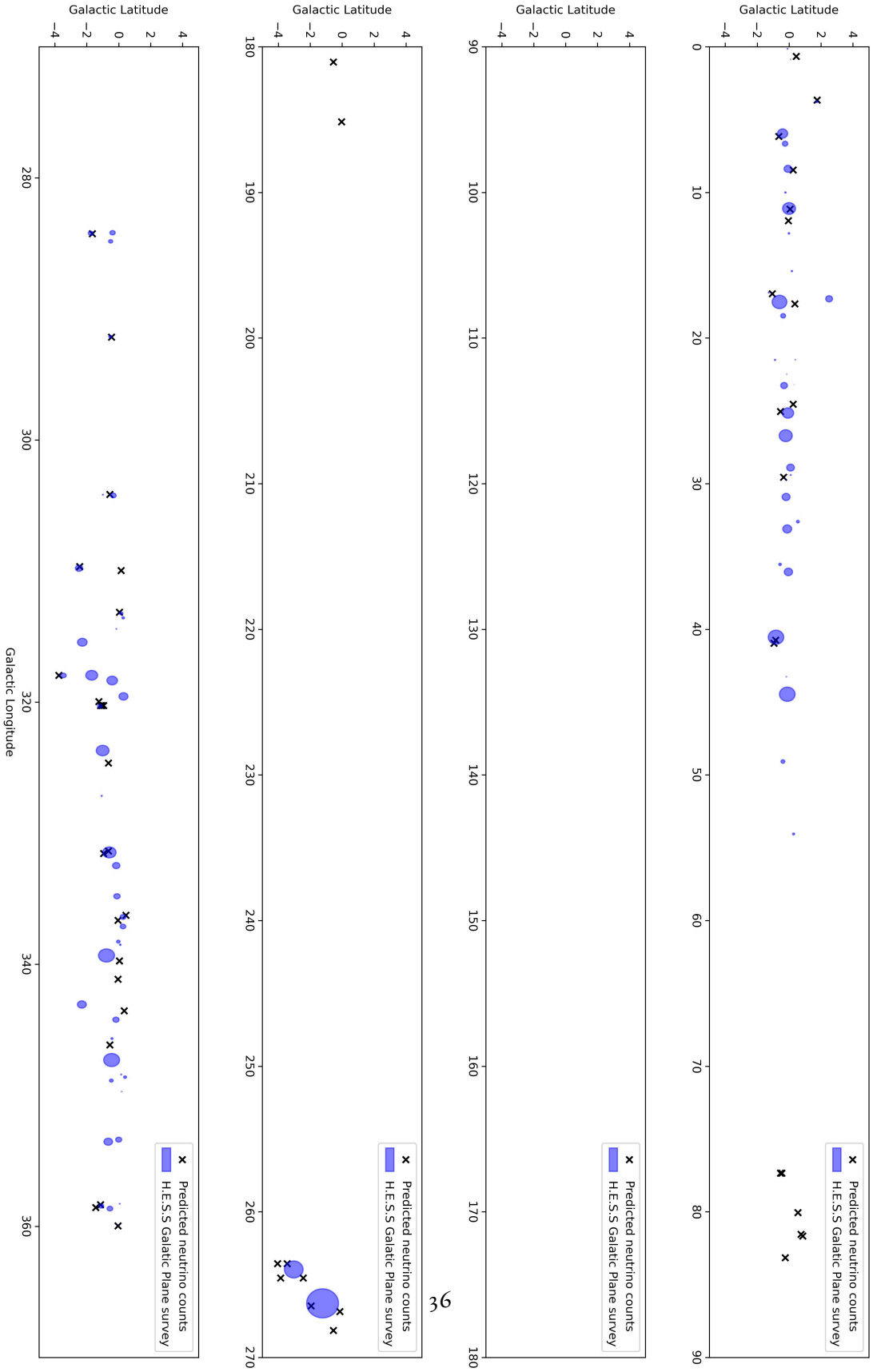

Figure 4.12: Expected neutrino counts with ANTARES for one of the populations. The blue sources with extension represent the H.E.E.S sources

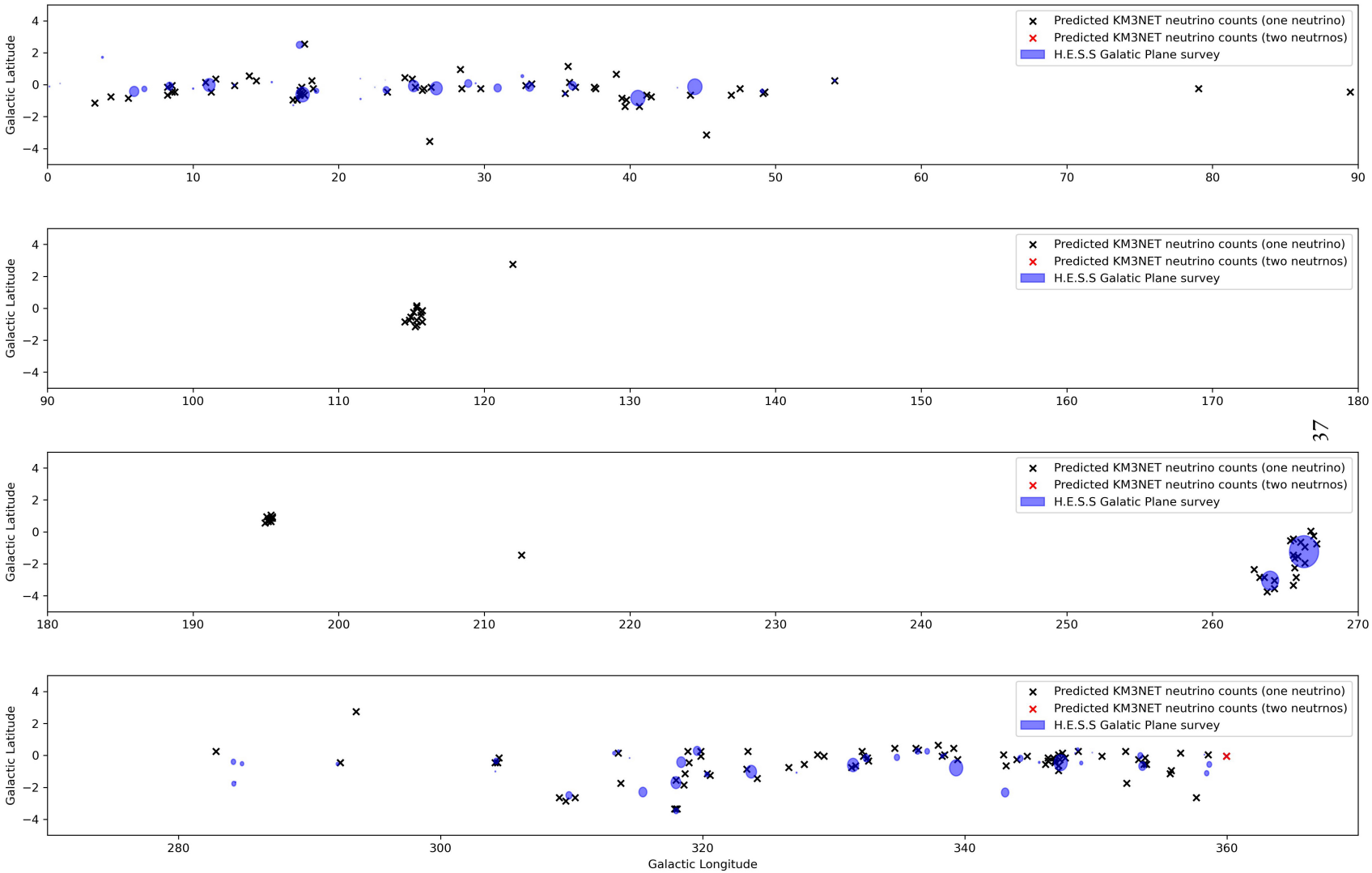

Figure 4.13: Expected neutrino counts with KM3NeT for one of the populations. The blue sources with extension represent the H.E.S sources

5

Summary and Conclusion

This master thesis centered on predicting potential neutrino emission within our galaxy, offering valuable insights into the origin of cosmic rays. Neutrinos and gamma rays can be produced simultaneously in pp interactions. This implies that if gamma rays are of hadronic origin, they are undoubtedly accompanied by the production of neutrinos. By establishing a correlation between the gamma-ray and neutrino spectra, we aim to identify potential neutrino sources in our galaxy.

We developed our model under the assumption of gamma rays to be purely hadronic in origin. We have utilized 3000 very high energy gamma ray populations. The populations consists of a total of 831 sources per population, with 78 of them corresponding to sources in the H.E.S.S. galactic plane survey, while the remaining sources were simulated. We assumed the energy spectrum for these sources follows a power-law model with a spectral index of 2.3 within the energy range of 1 to 100 TeV. Subsequently, we applied our developed model to predict the associated neutrino emissions.

Consequently, we generated skymaps to visualize the flux of the predicted sources and their spatial distribution across the galactic plane (see Figures 4.1, 4.2, 4.3). To validate the accuracy of our model and investigate the spatial correspondence between the predicted sources and observed events, we conducted a comparison with observed neutrino events from the ANTARES neutrino detector. We utilized eleven years of ANTARES data, spanning January 2007 to December 2017, resulting in a total livetime of 3136 days. The dataset comprised a substantial number of track-like events, in total 8754 events. As the ANTARES data observes the entire sky, while our skymaps focused solely on the galactic plane, we needed to establish the spatial correspondence between the ANTARES data points and the pixels in our skymaps. A total of 747 events fulfilled the requirements for spatial agreement between the ANTARES data and the skymap pixels.

In order to compare our predicted neutrino sources with the ANTARES data, we needed to estimate the ex-

pected counts based on our model. The total observation time spanned 11 years, resulting in a combined integration time of 27×10^7 seconds. The solid angle, was determined from the skymaps, with each bin on the map corresponding to 0.1 degrees. Utilizing this information, we calculated the expected counts for each source in our model. The same process was repeated for KM3NeT, employing the same observation time and but different effective area of this telescope.

We proceeded to generate count plots for each population to provide a visual representation of our results (see Figures 4.12 and 4.13). The majority of our sources yielded no neutrino counts, while the remaining sources had a count of one. In the case of KM3NeT, a few sources were expected to have two neutrino counts. On average, we found a total of 54 predicted counts for ANTARES and 222 counts for KM3NeT. This aligns with our expectation that our model only accounts for astrophysical neutrinos, while neutrino telescopes such as ANTARES also detect atmospheric neutrinos, resulting in a higher total count. Therefore, it was anticipated that our predictions would be smaller than the actual event counts recorded by ANTARES, which amounted to 747.

It is important to note that while the 747 events observed by ANTARES in the galactic plane provide valuable insights into the spatial distribution of neutrino events, it is not conclusive evidence that they solely originate from galactic sources based solely on their spatial positions. In fact, the lack of clustering among these events suggests that there are hardly any Galactic neutrinos among them. To establish a concrete association between the observed neutrino events and their source origins, further analysis and investigations are required.

The potential for improving the correspondence between the observed and predicted neutrino events lies in the prospects of future neutrino telescopes with enhanced capabilities. Advancements in technology and the development of more sensitive detectors offer promising opportunities to gather higher-quality data, can lead to improved accuracy in discovering the sources of neutrinos.

Also, in our study we have primarily focused on the assumption of an exclusively hadronic origin for the observed gamma-ray sources. However, it is crucial to acknowledge that some gamma-ray sources in the universe are dominated by leptonic emission processes. This implies that in these cases, the correlation between gamma rays and neutrinos may not hold to the same extent as in hadronic-dominated sources. Future investigations may need to consider the interplay between these different emission mechanisms for a more comprehensive understanding of the neutrino production in various astrophysical sources. Our analysis has primarily concentrated on predicting neutrino emissions from discrete astrophysical sources. Nevertheless, it is essential to recognize that diffuse emission also contributes to the overall neutrino flux.

Lastly, in the course of conducting this research, it is noteworthy to mention that a recent paper from the IceCube Collaboration, titled '[Observation of high-energy neutrinos from the Galactic plane] [44],' has been published subsequent to the completion of this thesis. This paper represents the latest state-of-the-art research about the galactic neutrinos. Regrettably, due to the timing of its release, we were unable to incorporate a detailed comparison of our work with the insights presented in this new research. Nevertheless, this paper offers a promising avenue for future investigations, as the findings therein may serve as a valuable reference point for further studies in this domain.

In conclusion, this thesis sets the stage for further exploration and advancements in the field of neutrino astrophysics. The pursuit of unraveling the mysteries surrounding the origin of neutrinos and their connections to cosmic rays is an exciting and challenging journey that promises to unveil new insights into the nature of the universe we inhabit.

References

[1] R. Batzofin and N. Komin, "Predicting neutrino emission for the sources in the h.e.s.s. galactic plane survey," in *Proceedings of 37th International Cosmic Ray Conference — PoS(ICRC2021)*. Sissa Medialab, jul 2021. [Online]. Available: https://doi.org/10.22323%2F1.395.0996

[2] M. Tanabashi, K. Hagiwara, K. Hikasa, K. Nakamura, and e. a. Sumino, "Review of particle physics," *Phys. Rev. D*, vol. 98, p. 030001, Aug 2018. [Online]. Available: https://link.aps.org/doi/10.1103/PhysRevD.98.030001

[3] C. Bigongiari, "The km3net project for a very large submarine neutrino telescope." *Ad Hoc Sensor Wireless Networks*, vol. 8, pp. 119–140, 01 2009.

[4] A. Albert, M. Andrv©, M. Anghinolfi, M. Ardid, and J.-J. et al., "Joint constraints on galactic diffuse neutrino emission from the antares and icecube neutrino telescopes," *The Astrophysical Journal Letters*, vol. 868, no. 2, p. L20, nov 2018. [Online]. Available: https://dx.doi.org/10.3847/2041-8213/aaeecf

[5] J. Carr, D. Dornic, F. Jouvenot, U. F. Katz, S. Kuch, G. Maurin, and R. Shanidze, "Sensitivity studies for the cubic-kilometre deep-sea neutrino telescope km3net," 2007.

[6] "Data set for the 2007-2017 antares search for cosmic neutrino point sources," https://antares.in2p3.fr/data-set-for-the-2007-2017-antares-search-for-cosmic-neutrino-point-sources/, accessed on May 28, 2023.

[7] C. D. Anderson, "The Apparent Existence of Easily Deflectable Positives," *Science*, vol. 76, pp. 238–239, 1932.

[8] Y. Shikaze, S. Haino, K. Abe, H. Fuke, T. Hams, K. Kim, and et al., "Measurements of 0.2–20gev/n cosmic-ray proton and helium spectra from 1997 through 2002 with the BESS spectrometer," *Astroparticle Physics*, vol. 28, no. 1, pp. 154–167, sep 2007. [Online]. Available: https://doi.org/10.1016%2Fj.astropartphys.2007.05.001

[9] A. D. Panov, J. H. Adams, H. S. Ahn, G. L. Bashinzhagyan, J. W. Watts, J. P. Wefel, J. Wu, O. Ganel, T. G. Guzik, V. I. Zatsepin, I. Isbert, K. C. Kim, M. Christl, E. N. Kouznetsov, M. I. Panasyuk, E. S. Seo, N. V. Sokolskaya, J. Chang, W. K. H. Schmidt, and A. R. Fazely, "Energy spectra of abundant nuclei of primary cosmic rays from the data of ATIC-2 experiment: Final results," *Bulletin of the Russian Academy of Sciences: Physics*, vol. 73, no. 5, pp. 564–567, may 2009. [Online]. Available: https://doi.org/10.3103%2Fs1062873809050098

[10] Y. S. Yoon, H. S. Ahn, P. S. Allison, M. G. Bagliesi, and et al., "COSMIC-RAY PROTON AND HELIUM SPECTRA FROM THE FIRST CREAM FLIGHT," *The Astrophysical Journal*, vol. 728, no. 2, p. 122, jan 2011. [Online]. Available: https://doi.org/10.1088%2F0004-637x%2F728%2F2%2F122

[11] O. Adriani, G. C. Barbarino, G. A. Bazilevskaya, and et al., "TIME DEPENDENCE OF THE PROTON FLUX MEASURED BY PAMELA DURING THE 2006 JULY-2009 DECEMBER SOLAR MINIMUM," *The Astrophysical Journal*, vol. 765, no. 2, p. 91, feb 2013. [Online]. Available: https://doi.org/10.1088%2F0004-637x%2F765%2F2%2F91

[12] M. Aguilar and e. a. Aisa, "Precision measurement of the proton flux in primary cosmic rays from rigidity 1 gv to 1.8 tv with the alpha magnetic spectrometer on the international space station," *Phys. Rev. Lett.*, vol. 114, p. 171103, Apr 2015. [Online]. Available: https://link.aps.org/doi/10.1103/PhysRevLett.114.171103

[13] T. Antoni, "A non-parametric approach to infer the energy spectrum and the mass composition of cosmic rays," 2001.

[14] R. Abbasi *et al.*, "Highlights from the Telescope Array experiment," *PoS*, vol. ICRC2021, p. 012, 2022.

[15] A. Aab and A. et al., "Measurement of the cosmic-ray energy spectrum above 2.5×10^{18} eV using the pierre auger observatory," *Phys. Rev. D*, vol. 102, p. 062005, Sep 2020. [Online]. Available: https://link.aps.org/doi/10.1103/PhysRevD.102.062005

[16] K. Greisen, "End to the cosmic-ray spectrum?" *Phys. Rev. Lett.*, vol. 16, pp. 748–750, Apr 1966. [Online]. Available: https://link.aps.org/doi/10.1103/PhysRevLett.16.748

[17] G. T. Zatsepin and V. A. Kuzmin, "Upper limit of the spectrum of cosmic rays," *JETP Lett.*, vol. 4, pp. 78–80, 1966.

[18] T. P. A. Collaboration, A. Aab, and P. A. et al., "The pierre auger observatory: Contributions to the 35th international cosmic ray conference (icrc 2017)," 2017.

[19] D. Caprioli, "Cosmic-ray acceleration in supernova remnants: non-linear theory revised," *Journal of Cosmology and Astroparticle Physics*, vol. 2012, no. 07, pp. 038–038, jul 2012. [Online]. Available: https://doi.org/10.1088%2F1475-7516%2F2012%2F07%2F038

[20] C. D. Dermer and B. Giebels, "Active galactic nuclei at gamma-ray energies," *Comptes Rendus Physique*, vol. 17, no. 6, pp. 594–616, jun 2016. [Online]. Available: https://doi.org/10.1016%2Fj.crhy.2016.04.004

[21] E. Waxman, "High energy neutrinos from gamma-ray bursts," *Nuclear Physics B - Proceedings Supplements*, vol. 91, no. 1-3, pp. 494–500, jan 2001. [Online]. Available: https://doi.org/10.1016%2Fs0920-5632%2800%2900980-4

[22] B. P. Abbott, R. Abbott, T. D. Abbott, and et al, "Gw170817: Observation of gravitational waves from a binary neutron star inspiral," *Phys. Rev. Lett.*, vol. 119, p. 161101, Oct 2017. [Online]. Available: https://link.aps.org/doi/10.1103/PhysRevLett.119.161101

[23] M. Aartsen and et al., "Neutrino emission from the direction of the blazar TXS 0506056 prior to the IceCube-170922a alert," *Science*, vol. 361, no. 6398, pp. 147–151, jul 2018. [Online]. Available: https://doi.org/10.1126%2Fscience.aat2890

[24] P. Cristofari, "The hunt for pevatrons: The case of supernova remnants," *Universe*, vol. 7, no. 9, p. 324, aug 2021. [Online]. Available: https://doi.org/10.3390%2Funiverse7090324

[25] A. Kheirandish and J. Wood, "Icecube search for galactic neutrino sources based on hawc observations of the galactic plane," 2019.

[26] A. D. Angelis and M. Mallamaci, "Gamma-ray astrophysics," *The European Physical Journal Plus*, vol. 133, no. 8, aug 2018. [Online]. Available: https://doi.org/10.1140%2Fepjp%2Fi2018-12181-0

[27] A. Kheirandish, "Identifying galactic sources of high-energy neutrinos," *Astrophysics and Space Science*, vol. 365, 06 2020.

[28] M. Aartsen, M. Ackermann, J. Adams, and et al., "The IceCube neutrino observatory: instrumentation and online systems," *Journal of Instrumentation*, vol. 12, no. 03, pp. P03 012–P03 012, mar 2017. [Online]. Available: https://doi.org/10.1088%2F1748-0221%2F12%2F03%2Fp03012

[29] A. Albert, M. André , M. Anghinolfi, and et al., "ANTARES and IceCube combined search for neutrino point-like and extended sources in the southern sky," *The Astrophysical Journal*, vol. 892, no. 2, p. 92, apr 2020. [Online]. Available: https://doi.org/10.3847%2F1538-4357%2Fab7afb

[30] M. Ageron, J. Aguilar, I. A. Samarai, and et al., "ANTARES: The first undersea neutrino telescope," *Nuclear Instruments and Methods in Physics Research Section A: Accelerators, Spectrometers, Detectors and Associated Equipment*, vol. 656, no. 1, pp. 11–38, nov 2011. [Online]. Available: https://doi.org/10.1016%2Fj.nima.2011.06.103

[31] KM3NeT Collaboration, "KM3NeT," https://www.km3net.org, Accessed 2023, accessed on May 18, 2023.

[32] T. K. Collaboration, S. Aiello, A. Albert, and et al., "Probing invisible neutrino decay with km3net/orca," *Journal of High Energy Physics*, vol. 2023, no. 4, p. 90, 2023. [Online]. Available: https://doi.org/10.1007/JHEP04(2023)090

[33] S. e. a. Aiello, "Sensitivity of the km3net/arca neutrino telescope to point-like neutrino sources," Apr 2019. [Online]. Available: https://www.sciencedirect.com/science/article/pii/S0927650518302809?via%3Dihub

[34] W. B. Atwood and A. A. A. et al., "THE LARGE AREA TELESCOPE ON THEiFERMI GAMMA-RAY SPACE TELESCOPE/iMISSION," *The Astrophysical Journal*, vol. 697, no. 2, pp. 1071–1102, may 2009. [Online]. Available: https://doi.org/10.1088%2F0004-637x%2F697%2F2%2F1071

[35] C. Steppa and K. Egberts, "Modelling the galactic very-high-energy i/i-ray source population," *Astronomy &amp Astrophysics*, vol. 643, p. A137, nov 2020. [Online]. Available: https://doi.org/10.1051%2F0004-6361%2F202038172

[36] H. Abdalla, A. Abramowski, F. Aharonian, and F. et al., "The h.e.s.s. galactic plane survey," *Astronomy &amp Astrophysics*, vol. 612, p. A1, apr 2018. [Online]. Available: https://doi.org/10.1051%2F0004-6361%2F201732098

[37] S. R. Kelner, F. A. Aharonian, and V. V. Bugayov, "Energy spectra of gamma rays, electrons, and neutrinos produced at proton-proton interactions in the very high energy regime," *Phys. Rev. D*, vol. 74, p. 034018, Aug 2006. [Online]. Available: https://link.aps.org/doi/10.1103/PhysRevD.74.034018

[38] V. Zabalza, "naima: a python package for inference of relativistic particle energy distributions from observed nonthermal spectra," 2015.

[39] V. N. Gribov and B. Pontecorvo, "Neutrino astronomy and lepton charge," *Phys. Lett. B*, vol. 28, p. 493, 1969.

[40] A. Donath, C. Deil, M. P. Arribas, J. King, E. Owen, R. Terrier, I. Reichardt, J. Harris, R. Bühler, and S. Klepser, "Gammapy - a python package for γ-ray astronomy," 2015.

[41] A. Albert, M. André , M. Anghinolfi, and et al., "Joint constraints on galactic diffuse neutrino emission from the ANTARES and IceCube neutrino telescopes," *The Astrophysical Journal*, vol. 868, no. 2, p. L20, nov 2018. [Online]. Available: https://doi.org/10.3847%2F2041-8213%2Faaeecf

[42] A. Albert, M. André , M. Anghinolfi, G. Anton, M. Ardid, and et al., "The search for neutrinos from TXS 0506056 with the ANTARES telescope," *The Astrophysical Journal*, vol. 863, no. 2, p. L30, aug 2018. [Online]. Available: https://doi.org/10.3847%2F2041-8213%2Faad8c0

[43] J. Aublin, G. Illuminati, and S. Navas, "Searches for point-like sources of cosmic neutrinos with 11 years of antares data," 2019.

[44] and R. Abbasi, M. Ackermann, J. Adams, and J. A. A. et al., "Observation of high-energy neutrinos from the galactic plane," *Science*, vol. 380, no. 6652, pp. 1338–1343, jun 2023. [Online]. Available: https://doi.org/10.1126%2Fscience.adc9818

Appendix

This chapter presents a collection of plots and maps that complement the main body of the thesis. These visuals provide additional insights into results and predictions discussed in earlier chapters. The description accompanying each plot provides context.

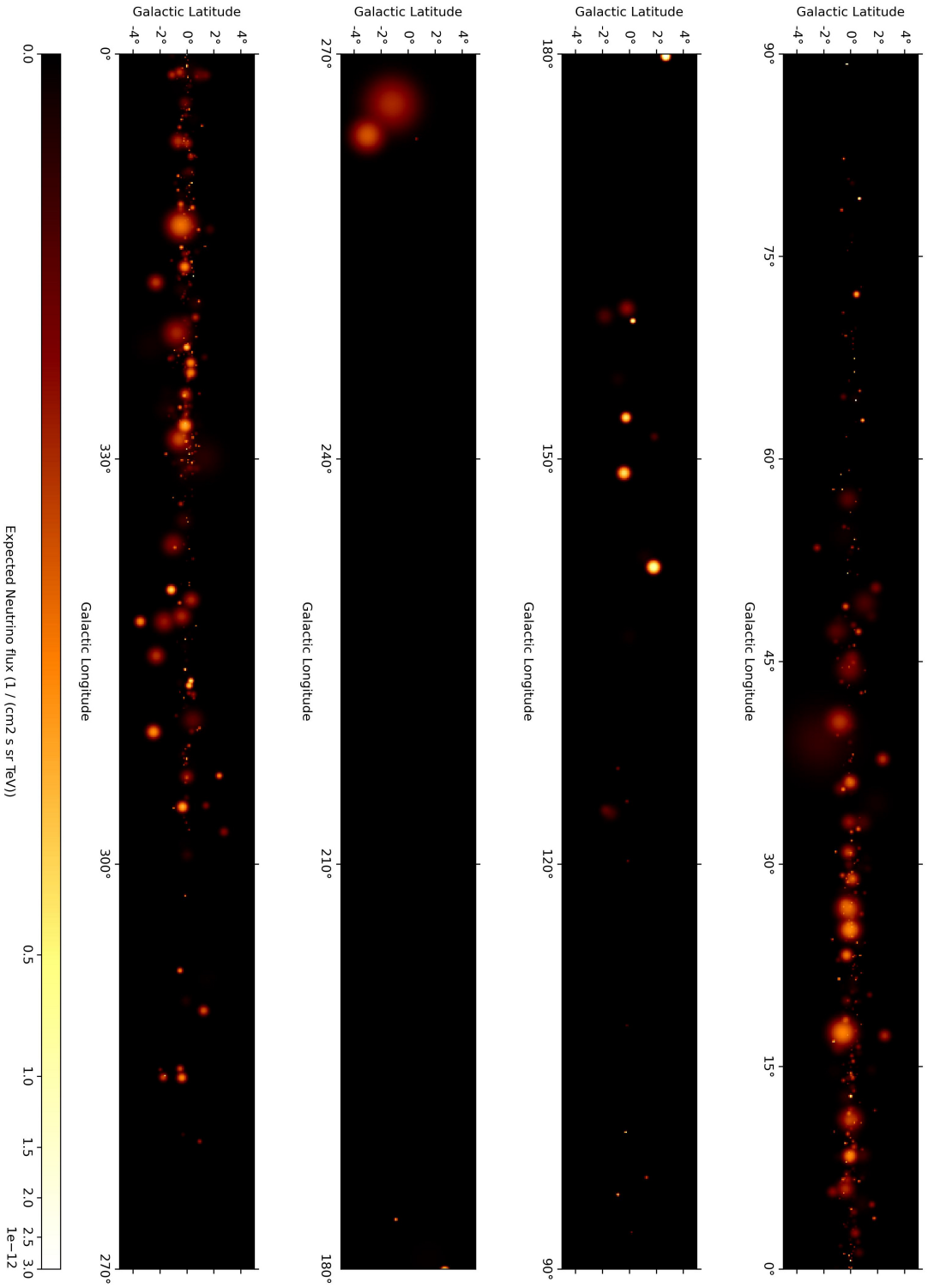

Figure 1: sky map for one of the sample populations showing neutrino sources and their flux in the energy bin of 95.5 to 100 TeV

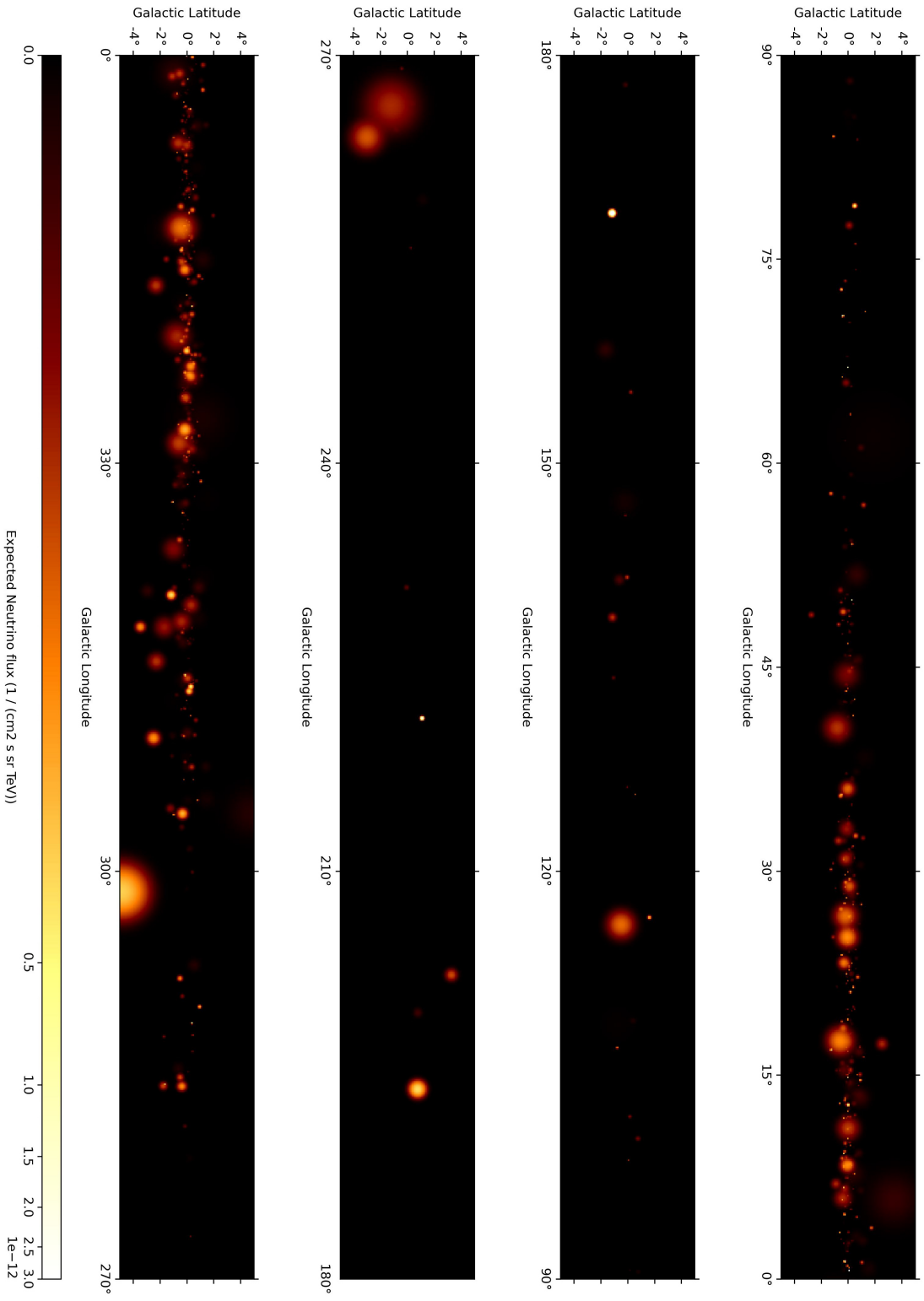

Figure 2: sky map for one of the sample populations showing neutrino sources and their flux in the energy bin of 95.5 to 100 TeV

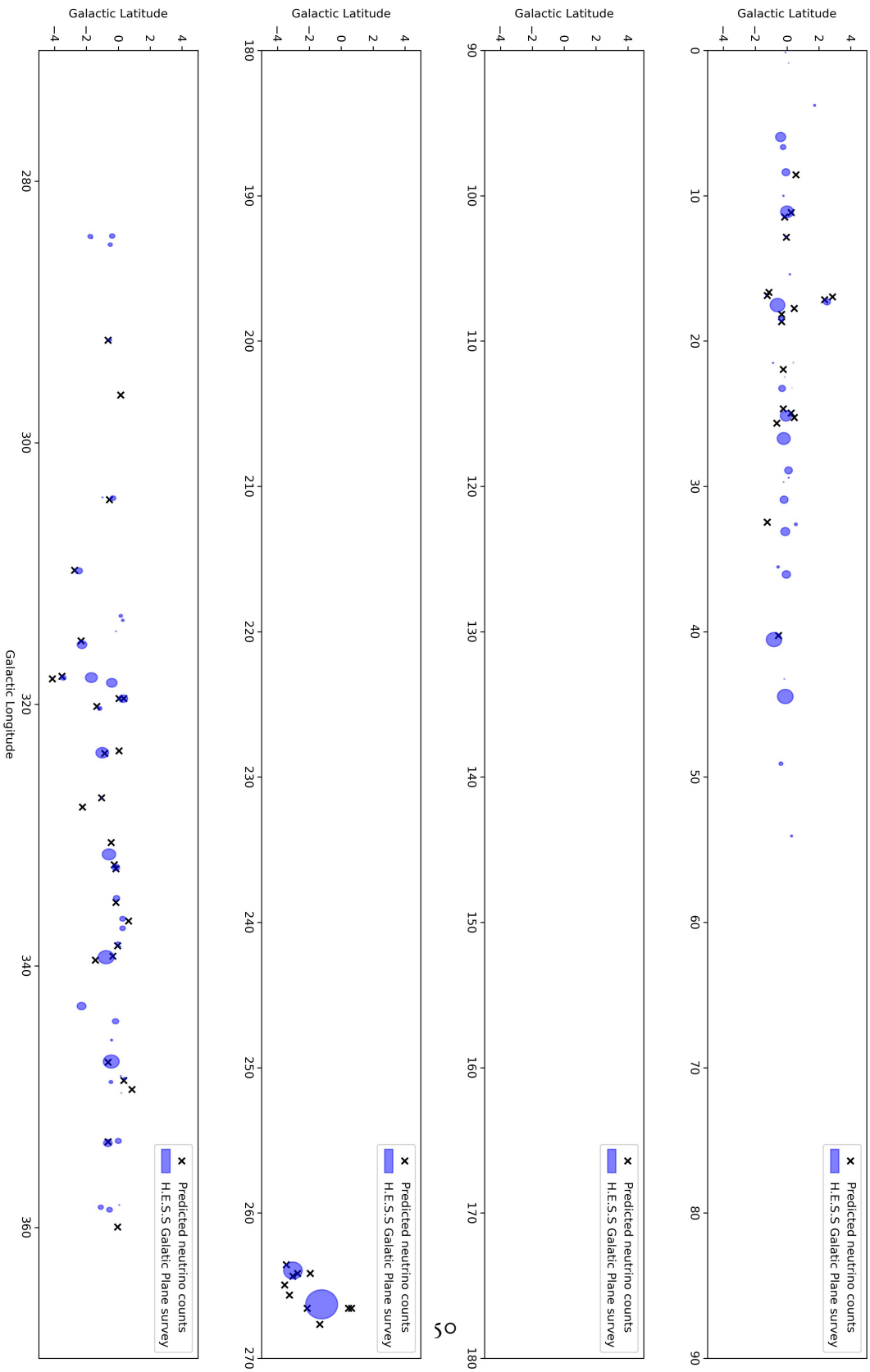

Figure 3: Expected neutrino counts with ANTARES for one of the populations. The blue sources with extension represent the H.E.S.S sources

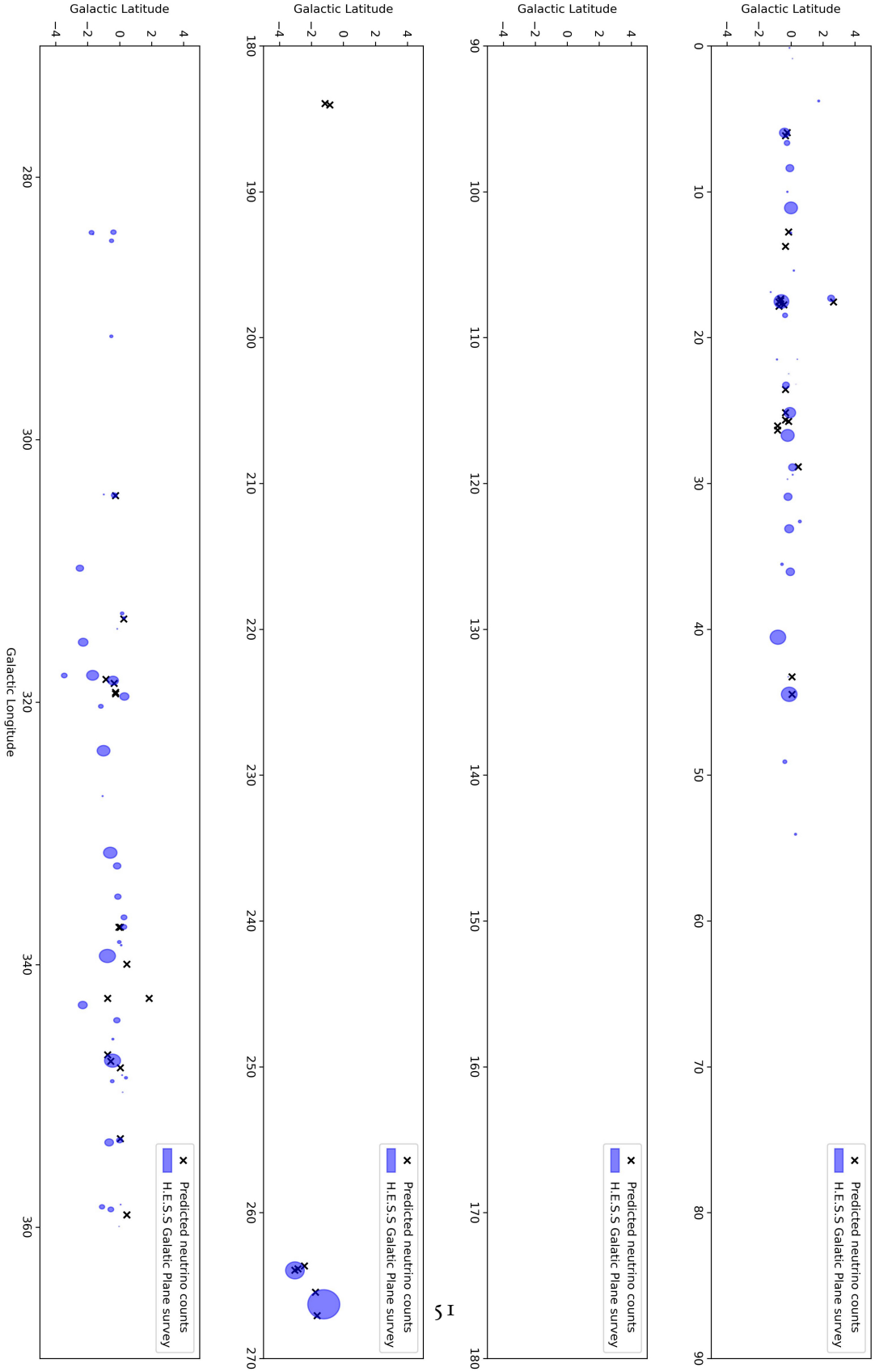

Figure 4: Expected neutrino counts with ANTARES for one of the populations. The blue sources with extension represent the H.E.S.S sources

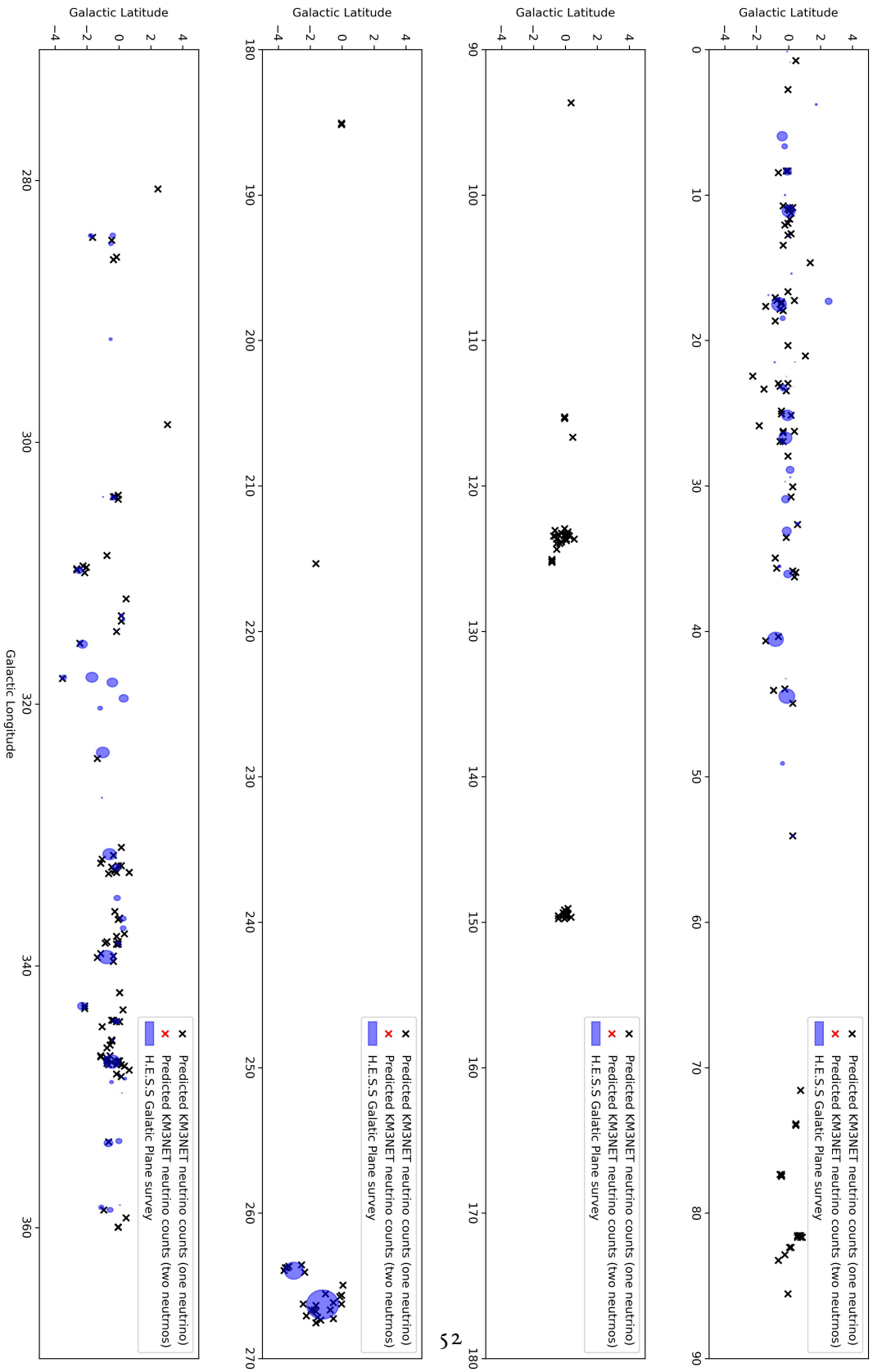

Figure 5: Expected neutrino counts with KM3NET for one of the populations. The blue sources with extension represent the H.E.S.S sources

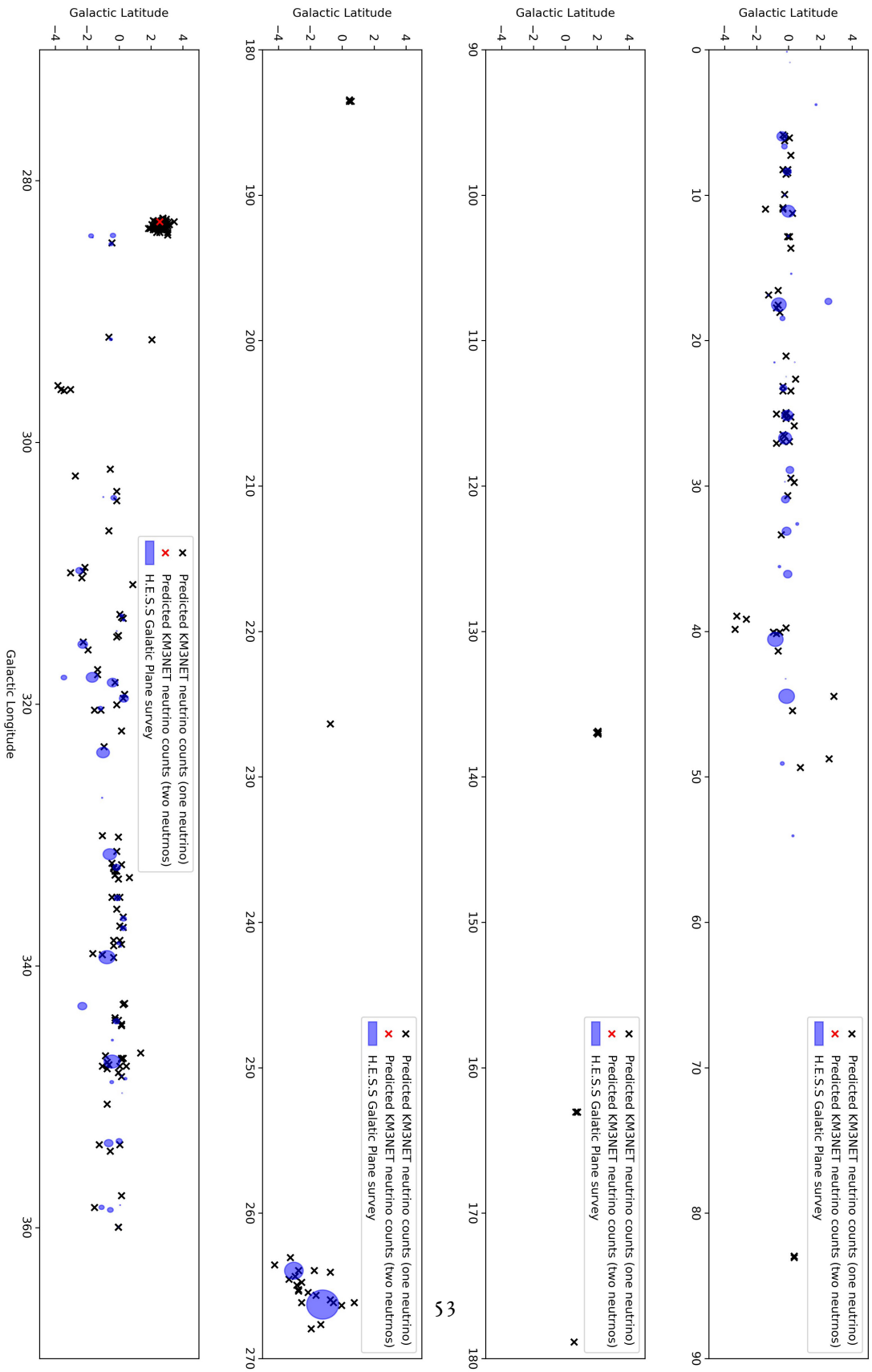

Figure 6: Expected neutrino counts with KM3NET for one of the populations. The blue sources with extension represent the H.E.S.S sources